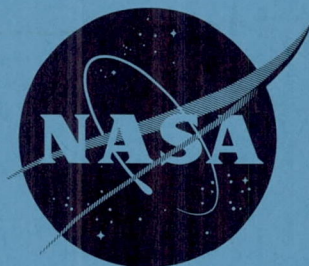


40p  
CONFIDENTIAL

679

NASA TM X-355

N63-14772  
CLASSIFICATION CHANGED TO  
DECLASSIFIED EFFECTIVE  
12 MARCH 63 AUTHORITY  
NASA CON 3 BY J.J. CARROLL



Code 1

# TECHNICAL MEMORANDUM

## X-355

AN EXPERIMENTAL STUDY OF THE FLUTTER OF SAILS  
HAVING A DELTA PLANFORM TESTED FROM A

MACH NUMBER OF 0.1 TO A

MACH NUMBER OF 1.9

By Robert W. Hess

Langley Research Center  
Langley Field, Va.

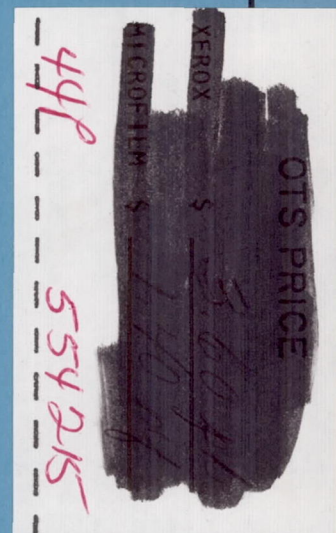
CLASSIFIED DOCUMENT - TITLE UNCLASSIFIED

This material contains information affecting the national defense of the United States within the meaning of the espionage laws, Title 18, U.S.C., Secs. 793 and 794, the transmission or revelation of which in any manner to an unauthorized person is prohibited by law.

NATIONAL AERONAUTICS AND SPACE ADMINISTRATION  
WASHINGTON

March 1961

CONFIDENTIAL



DECLASSIFIED

CONFIDENTIAL

NATIONAL AERONAUTICS AND SPACE ADMINISTRATION

TECHNICAL MEMORANDUM X-355

AN EXPERIMENTAL STUDY OF THE FLUTTER OF SAILS

HAVING A DELTA PLANFORM TESTED FROM A

MACH NUMBER OF 0.1 TO A

MACH NUMBER OF 1.9\*

By Robert W. Hess

SUMMARY

14772

Sails having a delta planform with a leading-edge sweep angle of  $55^\circ$  and a span of about 8 inches were fluttered through a range of angle of attack and dynamic pressure at subsonic speeds and transonic speeds. Larger sails with a span of about 18 inches were tested at a Mach number of 1.9. Two types of flutter were encountered during the tests, local flutter and full-sail flutter. Local flutter was confined to a small percentage of the total sail area whereas full-sail flutter involved the whole sail. For a given set of aerodynamic and structural conditions, flutter was found to occur when the angle of attack was reduced to a sufficiently low, positive value. In general, flutter occurred below an angle of attack of about  $2^\circ$  to  $4^\circ$  at very low dynamic pressures (10 lb/sq ft to 20 lb/sq ft) and below about  $10^\circ$  in the high dynamic-pressure range (120 lb/sq ft to 200 lb/sq ft). The angle of attack at flutter varied rapidly with dynamic pressure in the low dynamic-pressure range and approached a constant angle of attack in the high dynamic-pressure range. No effect of Mach number could be determined. The variation of the camber of the sails affected the angle of attack at which flutter occurred and obscured the interpretation of the results of tests designed to determine the effects of sail porosity and density. This type of lifting surface appears to be usable from a flutter standpoint with a limitation in the angle of attack.

#### INTRODUCTION

The problem of finding a light, controllable configuration for returning rocket booster stages and personnel capsules through the earth's

---

\*Title, Unclassified.

CONFIDENTIAL

03:10:29.1030

CONFIDENTIAL

atmosphere has resulted in a variety of proposals. A suggested method is the erectable structure; that is, the lifting surface is carried away from the earth in a collapsed condition to be erected prior to reentry. One structure of this type is the sail, with a lifting surface of a woven fabric or a membrane, which is characterized by low wing loadings and high values of lift and drag per unit weight. The analytical results of reference 1 (for a two-dimensional sail) indicate that lift-drag ratios in excess of 1 are possible.

The sail, however, is subject to a membrane type of flutter which must be considered when the conditions at which the vehicles must operate along the flight boundary are determined. A "flag waving" or "luffing" motion would be expected to occur when the loading on the sail is not sufficient to hold the sail in a taut attitude. This implies that, for a given set of aerodynamic and structural conditions, there would exist an angle of attack below which a possibly dangerous flutter condition might occur. Consideration of the optimum reentry trajectories of a low wing loading vehicle such as the sail indicates that operation at very high angles of attack would be required at orbital and hypersonic speeds but at low supersonic and transonic speeds operation at moderate angles of attack of the order of  $10^0$  would be required. Since the lowest required angles of attack occur at transonic and low supersonic speeds, it was considered desirable to investigate the limitations in angle of attack imposed by the flutter condition in this speed range.

This paper presents the results of an experimental study of the flutter characteristics of a series of delta planform sails. Subsonic and transonic characteristics were studied in the Langley 2-foot transonic aeroelasticity tunnel and the low supersonic speed range was investigated at a Mach number of 1.9 in the Langley 4- by 4-foot supersonic pressure tunnel.

#### SYMBOLS

a	speed of sound, ft/sec
f	flutter frequency, cps
M	Mach number
$p_t$	stagnation pressure, lb/sq ft
$p_{t,av}$	average stagnation pressure, lb/sq ft
q	dynamic pressure, lb/sq ft

CONFIDENTIAL

DECLASSIFIED

CONFIDENTIAL

3

R radius, in.  
 $T_t$  stagnation temperature,  $^{\circ}\text{R}$   
 $\alpha$  angle of attack, deg  
 $\rho$  air density, slugs/cu ft

### MODELS AND APPARATUS

Two families of models were tested in the Langley 2-foot transonic aeroelasticity tunnel and 4- by 4-foot supersonic pressure tunnel. All the models had delta planforms with leading-edge sweep angles of  $55^{\circ}$ . The models tested in the transonic tunnel had an area of 21.9 square inches; the models tested in the supersonic tunnel had a 65 percent larger span and had an area of 59.6 square inches. Because there were differences in the models and testing techniques, the adjectives small and large will be used to differentiate models and tests throughout the remainder of the report. Both tunnels in which the models were tested are continuous-flow tunnels capable of operating at stagnation pressures which are less than atmospheric pressure. The slotted-throat transonic tunnel is equipped to use either air or Freon-12, the latter being necessary to obtain sonic flow. Eight of the 11 models tested in this tunnel were tested in air at Mach numbers ranging from 0.093 to 0.869; the other three were tested in Freon-12 at Mach numbers ranging from 0.239 to 1.167. The adjustable nozzle blocks of the supersonic tunnel were set for a Mach number of about 1.9 for all the supersonic tests.

The structural components of the models, as shown in figures 1 to 4, consisted of an aluminum fuselage to which were attached the tapered aluminum trailing-edge spars and the compression spar. The cable which supported the leading edge of the sail was threaded through the tips of the fuselage and trailing-edge spars and attached to a tension screw on the compression spar at the rear of the model. As may be seen in figures 1 and 3, the spars were initially notched at the leading edge to obtain a desired stiffness distribution. Also, two spars (spars A and B) were constructed for each family of models to give a variation in the ratio of normal stiffness to chordwise stiffness. In addition, spar frequencies of four models were later reduced by cutting into the top of the spars at the root on one model and by adding weight to the tips of the spar of three models.

Initially, all models were tested with balsa leading- and trailing-edge spar fairings. However, the leading-edge spar fairings were often

CONFIDENTIAL

03171224.1030

CONFIDENTIAL

lost after being pushed up into the airstream by the billow in the sail and later models were generally tested with only the trailing-edge fairings.

Four fabrics were used as sails during the tests: nylon, rubberized nylon, Teflon, and fiberglass. As may be seen in table I, which lists the available fabric properties, these materials offered variation in porosity and density as well as undesirable variations in elongation.

The sail was folded over the steel cable along the leading edge and glued to the top and rear of the aluminum spar at the trailing edge. (See figs. 2 and 4.) The models were tested with the sail under the fuselage. The pretest tension in the sail could be reduced by screwing in the tension screw. A reverse procedure tightened the sail to a limited extent. Under no aerodynamic loads, tension could not be applied to the sail beyond the point where all the slack had been removed from the cables. Cable tension applied beyond this point served to reduce the sail camber when the sail was loaded aerodynamically since deflection normal to a cable is reduced by increased cable tension. The pretest sail tension was, therefore, dependent on the amount of tension in the fabric when it was attached to the cable and spars; in the case where the model had been previously tested, the pretest sail tension was also dependent on the amount that the fabric had stretched during the previous test. None of the sails were "drum head tight" before a test, the tightest sails being those that had all the slack removed.

The sail fabric, cable tension, and spar frequencies are listed for each model in table II. Zero cable tension in this table indicates the condition where the tension screw had been backed off to the point where the slack was removed from the cable.

#### Instrumentation

Two sets of two 60-ohm strain gages were mounted on all models, each set of gages being comprised of an active and a compensating gage. One set of gages was mounted at the trailing edge of one sail panel, the other at the root of one spar. (See figs. 2(a) and 4(a).) As might be expected, the strain gages on the sails were often destroyed early in the tests. The output signal was channeled through a 20-kilocycle amplifier to a recording oscillograph for direct observation and recording. The signal to response ratio of this system was flat to approximately 5,000 cycles per second. The signal from an accelerometer, mounted on the transonic-model sting as shown in figure 6, was also recorded on this system. Sample records from the small sail flutter tests are shown in figure 5.

CONFIDENTIAL

DECLASSIFIED

CONFIDENTIAL

5

Provisions had been made to measure forces and moments on the large models in the supersonic tunnel with a six-component balance; however, this balance was damaged at the beginning of the first test before supersonic flow was established.

The tunnel conditions at flutter (Mach number, density, stagnation pressure, and stagnation temperature) were recorded separately and are listed for each run in table III.

Motion pictures, with a frame speed of 1,000 frames per second, were taken of typical instability modes for each family of sails. Still photographs (fig. 6) were also taken of transonic model number 7 to record typical changes in sail camber as angle of attack and dynamic pressure were varied.

#### Test Procedure

Prior to testing, the model cables were set to a preselected tension; then, the model frequencies listed in table II were determined. The angle of attack at the start of each test was usually set above  $12^{\circ}$  unless previous tests indicated that a particular sail would not flutter at a lower angle. After the tunnel had been evacuated to the lowest desired stagnation pressure, the Mach number of the transonic tunnel was raised to the highest attainable Mach number and a record taken of existing vibrations. The angle of attack was then decreased slowly until one of the two observers noticed flutter. This procedure was repeated for two or more lower Mach numbers, after which the whole sequence was repeated at a higher stagnation pressure. At the higher stagnation pressures the limiting value of Mach number was determined by a dynamic pressure of approximately 200 pounds per square foot - a limitation based on the strength of the models. The procedure in the supersonic tunnel was the same except that the Mach number was essentially constant at about 1.9.

There were occasions in the transonic tunnel at the higher Mach numbers where the sails and supporting structure vibrated because of a tunnel disturbance. Since the onset of flutter was obscured by this motion, it was sometimes necessary to pass into the flutter range more than once to determine the angle of attack at which flutter started.

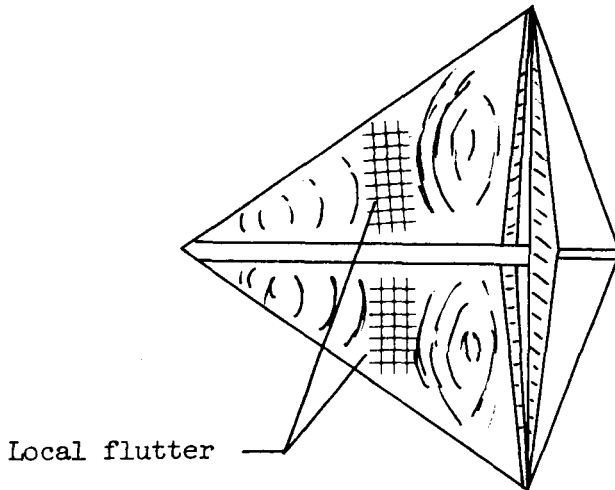
#### DISCUSSION OF RESULTS

Three types of instability were encountered during the transonic tests: local flutter, full-sail flutter, and static reversal. Local

CONFIDENTIAL



flutter was generally observed along the leading edge of the highly cambered portion of the sail and was confined to a small percentage of the total sail area. (See the following sketch.) At a given  $q$ , a



decrease in angle of attack below the initial instability angle increased the flutter amplitude and area over which it occurred. Full-sail flutter, which involved the whole sail, often started abruptly when a slight change in model angle of attack precipitated a change from local to full-sail flutter. Other models burst into full-sail flutter without this transition from local flutter. Static reversal, where the sail went from a positive camber to a negative camber, occurred only at very low dynamic pressures. The change from positive to negative camber was sudden and violent for some models whereas for other models the action was mitigated by a short burst of sail flutter preceding the reversal.

Changes in dynamic pressure and angle of attack were accompanied by changes in sail camber as shown in figures 6 and 7. Photographs of small model number 7 at two angles of attack are shown in figure 6. In addition to Mach number and dynamic pressure, two values of angle of attack are given for each photograph. One angle  $\alpha_{\text{flutter}}$  gives the angle of attack at which the model fluttered. The other angle  $\alpha_{\text{photograph}}$  gives the angle of attack of the model when the photographs were taken at the given values of Mach number and dynamic pressure. Figure 7 is a schematic drawing of the changes in camber drawn from the motion pictures taken during the small model tests. As may be noted in these figures, the sail gradually assumed an S-shape, the point of inflection and the positive cambered pattern of the sail moving rearward toward

DECLASSIFIED

CONFIDENTIAL

7

the trailing-edge spar with decreasing angle of attack. The maximum amplitude of the positive-cambered portion of the sail gradually decreased whereas the amplitude of the negative-cambered portion gradually increased until that portion of the sail was forced down and was no longer in contact with the fuselage.

No observations on the camber of the large models in the supersonic tunnel could be made since only the planform of the model and not the profile was observed from the tunnel side wall. This orientation of the large models (spar normal to the nozzle blocks) was necessary to minimize the transient forces on the sail due to turbulence that existed in the tunnel before the flow became supersonic.

The results of the tests are presented in table III for each model. Included in the tables are tunnel conditions at instability, angle of attack, spar and sail frequencies, and comments on the type of instability that was encountered. Additional comments on the condition of the sail before and after the tests are also presented in footnotes pertaining to each model. The results obtained from eight of the small models and six of the large models are plotted in figures 8 to 11 for angle of attack as a function of dynamic pressure. For comparative purposes the results of three of the small, nylon-covered models are plotted for angle of attack as a function of Mach number. The small-model data are coded to indicate the test sequence and average stagnation pressure. Local flutter, full-sail flutter, and reversal are designated by open symbols, solid symbols, and flagged symbols, respectively. The large-model data, figure 11, are coded by model number only.

The most consistent small-model results were obtained from the nylon-covered models (models 1, 2, and 3) which are plotted with angle of attack at the onset of flutter as a function of both dynamic pressure and Mach number in figure 8. A comparison of the two sets of curves indicates that, for the Mach number range in which the models were tested, the angle of attack at the onset of local flutter is a function of dynamic pressure and is essentially independent of Mach number. At low dynamic pressures in the neighborhood of 10 pounds per square foot, the angle of attack at flutter was about  $4^{\circ}$ . The angle of attack increased with increasing dynamic pressure to about 50 pounds per square foot; above this value the angle of attack gradually became asymptotic to an angle of about  $9^{\circ}$ .

The tension or, conversely, the lack of tension in the sail appeared to have a large effect on the angle of attack at the onset of flutter, but, since no consistent or accurate measurements could be taken of the amount of slack in the sails, no direct quantitative assessment of this effect can be made. However, it is possible to make some general observations from the test results.

CONFIDENTIAL



03:71:23:4.13:34

CONFIDENTIAL

The possible effects of increasing slack in the sails may be noted in figure 8, where the angle of attack at flutter for the same model and dynamic pressure increased with each successive test. This may be due to sail and/or cable stretching with increasing exposure to aerodynamic loading. The influence of sail slack or sail billow is most discernible when the results in figures 9(a) and 9(b) and 10(a) and 10(b) which are plots of results for small, Teflon-covered models without and with cable tension and small, rubber-coated-nylon models without and with cable tension, respectively, are compared. In both sets of tests the onset of flutter at dynamic pressures above 80 pounds per square foot occurred at lower angles of attack for the model with cable tension. Moreover, the sails with cable tension appeared to flutter within a band of angles of attack that was independent of dynamic pressure. It may also be noted that, at the values of dynamic pressure below 80 pounds per square foot, the results for the models with cable tension appear to be roughly the same as those tested without cable tension. This effect may be due to the fact that at lower dynamic pressures and angles of attack the normal forces on the cable were not large enough to cause significantly larger deflections on the cables that were not preloaded.

As was discussed in a previous section, the amount of billow in the sail was also dependent on the tension in the fabric when it was initially attached to the model frame. Some of the scatter in the results from the two families of sails may be due to a lack of control of the sail tension when the model was covered and also to changes in the sail during the tests. Two of the small Teflon models were identical. Model 7 was model 6 with tension in the cables; the third model was one that had been re-covered with Teflon. The test results from the three models are plotted in figures 9(a), 9(b), and 9(c). The results from models 6 and 7 fall close to each other at low values of  $q$  whereas the results from model 8 fall from  $1-1/2^\circ$  to  $3^\circ$  lower.

The results of the two large, nylon models (models 12 and 13), which were different sails, exhibit a much larger discrepancy than was encountered on any other tests. This difference in angles of attack at the onset of flutter was increased as small tears developed at the trailing edge of the sail of model number 13; a repeat of the first point in the sequence fluttered at an angle of attack that was  $2^\circ$  higher than when the sail was undamaged.

The effects of mass and porosity are difficult to assess primarily because of the previously discussed effects of camber. The only observable differences in the results are between the lighter nylon sails and the heavier, less elastic Teflon and rubberized-nylon sails. The nylon sails fluttered at higher angles of attack and the results are more consistent than those obtained from the heavier sails. The heavier sails (except for the fiberglass sail, model 11, from which very little data were obtained) also experienced full-sail flutter over a much wider range

CONFIDENTIAL

DECLASSIFIED

CONFIDENTIAL

9

of dynamic pressures. At a given dynamic pressure, local flutter on the nylon sails was encountered over a range of angles of attack before full-sail flutter developed, whereas the heavier sails generally burst into full-sail flutter without passing through this range of local flutter.

Only fragmentary information is presented on the flutter frequencies of the sails, since the sail strain gages on the transonic models were often lost early in the tests and all the sail strain gages on the supersonic sails were lost before the flow stabilized. In addition, the response from the gages that did remain were not always periodic but had a random response with no predominant frequency. One record taken at full-sail flutter and two records taken at local flutter are presented in figures 5(a), 5(b), and 5(c). The available measurements of the frequencies of the sails and spars at flutter are listed for each model in table III. There was no apparent change in the sail flutter that could be attributed to the variation in the spar frequencies.

As a matter of interest, the frequencies obtained from strain gages mounted on the sails of the small models at local flutter are plotted as a function of dynamic pressure on a log-log basis in figure 12. The straight line faired through the data is based on an estimate determined from the least-squares criteria. (See ref. 2.) In figure 12, the sum of the squares of the difference between the logarithm of the experimental frequencies and that of the line are a minimum. The fact that the least-squares analysis yielded an exponent of dynamic pressure near one-half suggests the possibility that the frequency may vary directly with velocity. However, similar examination of the variation of frequency with velocity indicates that the data for different densities tend to yield separate curves and therefore it appears that the dynamic pressure is the predominant variable.

## CONCLUSIONS

An investigation was made of the flutter of sails at subsonic, transonic, and supersonic speeds. The investigation indicated the following conclusions:

1. At high angles of attack, the model sails were stable. As the angle of attack was reduced, three types of instability were encountered: local flutter, full-sail flutter, and static reversal.

2. The angle of attack at the onset of local flutter and the flutter frequency are functions of dynamic pressure at subsonic and transonic speeds and are essentially independent of Mach number.

CONFIDENTIAL

03:41:28.1030

10

CONFIDENTIAL

3. At a given dynamic pressure, increasing the tension in the sail tended to increase the flutter-free range of angle of attack.

Langley Research Center,  
National Aeronautics and Space Administration,  
Langley Field, Va., July 29, 1960.

#### REFERENCES

1. Daskin, Walter, and Feldman, Lewis: The Characteristics of Two-Dimensional Sails in Hypersonic Flow. Jour. Aero. Sci., vol. 25, no. 1, Jan. 1958, pp. 53-55.
2. Hoel, Paul G.: Introduction to Mathematical Statistics. Second ed., John Wiley & Sons, Inc., c.1954.

CONFIDENTIAL

CONFIDENTIAL

CONFIDENTIAL

11

TABLE I.- MATERIAL PROPERTIES OF SAIL FABRICS

Material	Weight, oz/sq yd	Thickness, in.	Air permeability,* cu ft/min/sq ft	Ultimate elongation (minimum), percent		Tensile strength (minimum), lb/in.	
				Warp	Fill	Warp	Fill
Nylon (ripstop)	1.1	0.0032	80 to 120	22	22	40	40
Rubber-coated - nylon (ripstop)	3.0	.0042	0	----	----	155	110
Teflon	4.92	.0057	35 to 40	19.8	19.5	77.5	68.2
Fiberglass	3.0	.004	-----	----	----	125	200

\*Permeability - volume of air in cubic feet that will flow through 1 square foot of cloth in 1 minute. Air pressure at 1/2 inch of water.

CONFIDENTIAL

03:41:28.1030

12

CONFIDENTIAL

TABLE II.- MODELS TESTED

## (a) Small models

Model	Material	Cable tension, lb	Spar frequencies, cps		Test medium	Spar
			Symmetrical	Antisymmetrical		
1	Nylon	0	625	540	Air	A
2	Nylon <sup>1</sup>	0	386	265	Air	A
3	Nylon <sup>1,2</sup>	0	386	265	Freon	A
4	Nylon <sup>2</sup>	0	625	500	Air	A
5	Nylon <sup>3,2</sup>	0	398	512	Air	B
6	Teflon	0	628	508	Air	A
7	Teflon <sup>2</sup>	19.5	643	507	Air	A
8	Teflon <sup>2</sup>	0	584	480	Freon	A
9	Rubberized nylon	0	645	526	Air	A
10	Rubberized nylon <sup>2</sup>	19.5	650	475	Air	A
11	Fiberglass <sup>2</sup>	0	584	518	Freon	A

## (b) Large models

Model	Material	Cable tension, lb	Spar frequencies, cps		Spar
			Symmetrical	Antisymmetrical	
12	Nylon <sup>2</sup>	0	310	192	B
13	Nylon <sup>1,2</sup>	0	221	130	B
14	Teflon <sup>2</sup>	14	308	211	A
15	Rubberized nylon	0	324	184	A
16	Rubberized nylon <sup>2</sup>	0	318	187	A

<sup>1</sup>Spar frequency reduced by adding weight to spars.

<sup>2</sup>No balsa leading-edge spar fairing at start of test.

<sup>3</sup>Spar frequency reduced by notching spars at root.

CONFIDENTIAL

TABLE III.- FLUTTER TEST RESULTS

(a) Small-model tests

Run	Angle of attack, $\alpha$ , deg	$q$ , lb/sq ft	Mach number	$a$ , ft/sec	$P_t$ , lb/sq ft	$T_t$ , Or	$\rho$ , slugs/cu ft	Flutter frequency, cps		Remarks
								Sail	Spar	
Model 1 <sup>a</sup> ; nylon, no cable tension										
1	2.4	5.80	0.156	1,128	338	531.2	0.00377	375		Local flutter on forward slope of positive-cambered portion of sail
2	7.3	30.57	.378	1,120	348	536	.000342	575		Local flutter on forward slope of positive-cambered portion of sail
3	8.8	58.99	.534	1,113	358	543.5	.000334	950		Local flutter on forward slope of positive-cambered portion of sail
4	9.4	79.01	.624	1,112	374	552.4	.000328	1,000		Local flutter on forward slope of positive-cambered portion of sail, port side only
5	9.9	114.95	.796	1,102	391	568	.000299			Local flutter on forward slope of positive-cambered portion of sail, port side only
6	8.7	51.64	.845	1,094	165	568	.000121	782		Local flutter on forward slope of positive-cambered portion of sail, port side only
7	8.3	45.57	.770	1,106	162	568.4	.000126	714		Local flutter on forward slope of positive-cambered portion of sail, port side only
8	8.2	37.87	.684	1,116	158	565.9	.000130	600		Local flutter on forward slope of positive-cambered portion of sail, port side only
8	8									Full-sail flutter
9	7	24.24	.515	1,134	156	562.8	.000142	475		Local flutter on forward slope
9	4.9			1,134						Full-sail flutter
10	5.6	12.1	.352	1,146	152	559.1	.000149	220-450		Local-sail flutter
10	4.9	12.11	.351	1,146	153	558.8	.000150	330		Local-sail flutter
11	10.7	200.33	.681	1,128	840	578	.000680			Local flutter on forward slope of positive-cambered portion of sail
12	10.2	135.65	.536	1,142	819	573.5	.000723	1,100		Local flutter on forward slope of positive-cambered portion of sail
13	9.9	75.78	.589	1,151	794	566.8	.000756	700		Local flutter on forward slope of positive-cambered portion of sail, high cambered portion from 50 percent to 100 percent root chord
13	9.2	75.68	.589	1,151	795	567.1	.000757			Full-sail flutter
14	7.0	17.75	.183	1,159	775	562.8	.000789	330		Local flutter on forward slope of high positive-cambered portion of sail
14	6.3	18.80	.189	1,158	774	562.2	.000789			Full-sail flutter
15	10.4	200.32	.516	1,146	1,293	574.4	.001148	300-600		Local flutter on forward slope of high positive-cambered portion of sail; sail has S-shape
15	10.4									Full-sail flutter
16	10.6	126.12	.399	1,153	1,264	570.3	.001190			Local flutter on forward slope of high positive-cambered portion of sail
16	10.1	126.98	.401	1,153	1,265	570.3	.001191			Full-sail flutter; intermittent large amplitude
17	8.8	31.71	.195	1,160	1,232	563.5	.001246	520		Local flutter on forward slope of high positive-cambered portion of sail
17	8.4	31.66	.195	1,160	1,230	563.5	.001244			Full-sail flutter

<sup>a</sup>The sail was slightly wrinkled and had uneven sail tension distribution in some areas of the sail at the start of the tests.



CONFIDENTIAL

TABLE III.- FLUTTER TEST RESULTS - Continued

(a) Small-model tests - Continued

Run	Angle of attack, $\alpha$ , deg	$q$ , lb/sq ft	Mach number	$a$ , ft/sec	$P_t$ , lb/sq ft	$T_t$ , OR	$\rho$ , slugs/cu ft	Flutter frequency, cps		Remarks
								Sail	Spar	
Model 2 <sup>b</sup> ; nylon, no cable tension										
										Full-sail flutter
91	6.4	54.22	0.866	1,089	167	565.9	0.000122			Local flutter at leading edge of high cambered portion of sail
92	7.1	39.81	.693	1,113	162	563.1	.000134	875		Local flutter at leading edge of high cambered portion of sail
93	5.6	25.15	.507	1,132	167	559.7	.000153			Local flutter at leading edge of high cambered portion of sail
94	3.9	13.83	.373	1,141	157	556.5	.000153			Local flutter at leading edge of high cambered portion of sail
96	8.4	113.54	.850	1,103	368	574.9	.000271	1,250		Local flutter at leading edge of high cambered portion of sail
97	8.4	88.85	.696	1,121	360	573.0	.000292	1,100		Local flutter at leading edge of high cambered portion of sail
98	7.6	58.98	.543	1,136	348	567.6	.000310	950		Local flutter at leading edge of high cambered portion of sail
99	6.2	31.38	.382	1,146	340	562.2	.000327			Local flutter at leading edge of high cambered portion of sail
100	3.2	6.53	.170	1,156	330	558.8	.000338	217		Local flutter at leading edge of high cambered portion of sail
101	8.8	202.11	.705	1,124	808	578.0	.000643			Local flutter at leading edge of high cambered portion of sail
102	8.5	138.54	.559	1,140	785	573.5	.000683			Local flutter at leading edge of high cambered portion of sail
103	7.8	77.10	.403	1,149	762	566.8	.000721			Local flutter at leading edge of high cambered portion of sail
104	5.6	20.49	.202	1,157	742	561.3	.000754	413		Local flutter at leading edge of high cambered portion of sail
105	8.7	210.19	.528	1,139	1,295	569.0	.001161			Local flutter at leading edge of high cambered portion of sail
106	8.3	128.60	.403	1,148	1,268	565.9	.001201			Local flutter at leading edge of high cambered portion of sail
107	7.7	76.49	.306	1,153	1,250	562.8	.001233	1,050		Local flutter at leading edge of high cambered portion of sail
108	6.7	31.63	.194	1,155	1,235	558.8	.001260			Local flutter at leading edge of high cambered portion of sail

<sup>b</sup>A lead weight was added to the tip of each spar to reduce the span frequency. The tension in the sail appeared to be uniform in the sail before and after the test. The deflection normal to the sail was approximately 0.1 inch greater after the test.

CONFIDENTIAL

CONFIDENTIAL

CONFIDENTIAL

TABLE III.- FLUTTER TEST RESULTS - Continued

(a) Small-model tests - Continued

continued

Run	Angle of attack, $\alpha$ , deg	$q$ , lb/sq ft	Mach number	$a$ , ft/sec	$P_t$ , lb/sq ft	$T_t$ , OR	$\rho$ , slugs/cu ft	Flutter frequency, cps		Remarks
								Sail	Spar	
Model 3 <sup>c</sup> ; nylon, no cable tension										
134	8.4	203.19	0.585	498	1,279	519.0	0.004793	1,500	350	Local flutter, sail takes on S-shape
135	7.6	93.42	.380	501	1,249	518.4	.005144	900		Local flutter at leading edge of rear positive-cambered portion of sail
136	6.3	61.93	.306	502	1,243	517.6	.005266			Local flutter, area of local flutter extends rearward with decreasing $\alpha$
137	8.7	189.86	.780	503	775	528.7	.002470		260	Local flutter
138	8.3	121.47	.593	506	747	526.9	.002701	~1,300	330	Local flutter
139	7.2	61.21	.405	508	730	524.7	.002899			Local flutter
140	5.9	35.36	.305	509	714	523.3	.002940			Local flutter
141	9.1	157.60	1.156	508	434	553.2	.000914	~1,600	320	Local flutter
142	9.0	127.42	.997	512	392	548.4	.000979	1,300	400-450	Local flutter
143	8.4	94.37	.805	515	368	541.0	.001099	900	300	Local flutter
144	7.2	55.41	.586	518	347	537.0	.001202	700		Local flutter
145	5.7	26.13	.389	520	334	534.8	.001277	460	460	Local flutter
146	4.2	11.92	.260	521	326	532.6	.001304	315	315	Local flutter
147	2.6	11.94	.262	520	322	531.2	.001291	383	383	Full-sail flutter
148	8.7	76.61	1.152	514	210	545.2	.000437		350	Local flutter
149	7.5	44.70	.998	519	194	543.5	.000473			Local flutter
150	6.5	27.75	.769	524	185	537.4	.000551			Local flutter
151	4.9	11.81	.570	526	182	535.2	.000618	516	367	Local flutter
152	3.5	5.59	.357	529	177	533.0	.000664	340	516	Local flutter
152	2.1	5.59	.239	532	177	531.8	.000691		386	Local flutter
152			.259	532	177	531.8	.000691			Local flutter

This model was tested at

<sup>c</sup>This model was model 2 with no changes. The sail tension appeared to be uniform before and after the test.

CONFIDENTIAL

CONFIDENTIAL

TABLE III.- FLUTTER TEST RESULTS - Continued

(a) Small-model tests - Continued

Run	Angle of attack, $\alpha$ , deg	$q$ , lb/sq ft	Mach number	$a$ , ft/sec	$P_t$ , lb/sq ft	$T_t$ , OR	$\rho$ , slugs/cu ft	Flutter frequency, cps		Remarks
								Sail	Spar	
Model 4 <sup>d</sup> ; nylon, no cable tension										
86	12.4	158.09	0.594	1,133	810	571.1	0.000699		267	Local flutter at leading edge of high cambered portion of sail
87	10.4	159.75	.594	1,136	818	574.0	.000701		300	Local flutter at leading edge of high cambered portion of sail
88	10.4	159.86	.592	1,140	822	578	.000701		300	Local flutter at leading edge of high cambered portion of sail
89	10.5	163.66	.599	1,144	830	582.5	.000698			Local flutter at leading edge of high cambered portion of sail
90	10.7	152.38	.575	1,156	822	591.6	.000691		276-300	Local flutter at leading edge of high cambered portion of sail
Model 5 <sup>e</sup> ; nylon, no cable tension										
109	4.1	53.12	0.907	1,038	157	521	0.000120	~1,300	480	Local flutter
109	2.5	53.06	.903	1,042	158	524.7	.000120			Full-sail flutter
110	4.8	43.58	.776	1,060	154	523.9	.000129			Local flutter
110	2.5	43.94	.769	1,061	156	523.9	.000132	400	400	Full-sail flutter, starboard side
111	4.6	36.26	.672	1,071	155	519.3	.000140		337	Local flutter
111	2.7	36.26	.672	1,071	155	519.3	.000140		350	Full-sail flutter, starboard side
112	3.9	24.16	.519	1,090	154	519.3	.000151		550	Local flutter
112	2.9	24.23	.519	1,088	154	518.4	.000152			Full-sail flutter, starboard side
113	3.0	11.18	.337	1,102	152	515.5	.000162			Local flutter
113	2.1	11.18	.337	1,102	152	515.5	.000162			Full-sail flutter, starboard side
114	1.4	1.89	.135	1,109	150	512.4	.000169			Static reversal
115	7.5	123.43	.889	1,060	371	540.5	.000278			Local flutter, starboard side, billow on starboard twice that of port side
115	3.6	124.67	.894	1,059	373	540.0	.000278		500	Full-sail flutter
116	5.4	108.89	.782	1,079	363	542.7	.000292		800	Local flutter, starboard side only
116	4.6	103.71	.781	1,078	364	542.2	.000283		450	Full-sail flutter
117	6.4	80.03	.654	1,091	354	536.6	.000314			Local flutter
117	4.1	80.80	.659	1,091	354	537	.000313		~25	Full-sail flutter
118	6.0	57.31	.534	1,103	348	533.4	.000331			Local flutter, sail frayed near boom on starboard side

<sup>d</sup>This model was the same as model 1 except that the cloth had been shrunk to reduce the slack in the sail. The deflection normal to the sail (in down direction) increased from 0.15 inch before the test to 0.5 inch at the end of the test.

<sup>e</sup>The spars were notched at the root to reduce the spar frequencies. The tests were terminated after the cloth frayed along the trailing edge of the sail along the starboard spar fairing.

CONFIDENTIAL

CONFIDENTIAL

CONFIDENTIAL

17

TABLE III.- FLUTTER TEST RESULTS - Continued

(a) Small-model tests - Continued

Run	Angle of attack, $\alpha$ , deg	$q$ , lb/sq ft	Mach number	$a$ , ft/sec	$P_t$ , lb/sq ft	$T_t$ , OR	$\rho$ , slugs/cu ft	Flutter frequency, cps		Remarks
								Sail	Spar	
Model 6 <sup>f</sup> ; teflon, no cable tension										
31	4.3	52.59	0.854	1,092	165	567.6	0.000121		≈400	Full-sail flutter after model took static S-shape
32	4.4	38.21	.671	1,118	163	565.4	.000136		392	Full-sail flutter after model took static S-shape
33	3.3	24.33	.512	1,136	158	564.5	.000144		300	Full-sail flutter after model took static S-shape
34	2.7	12.02	.348	1,147	155	559.7	.000151		250	Full-sail flutter after model took static S-shape
35	2.1	0	0	1,158	154	557.2	.000161			Static instability, negative camber
35	7.4									Angle necessary to go from negative to positive camber
36	8.1	105.21	.825	1,108	344	578.9	.000252		520	Local flutter starboard, leading edge of positive cambered portion of sail
37	7.1	80.84	.689	1,126	334	577.1	.000269		417	Local flutter starboard, leading edge at quarter chord
38	4.5	53.57	.536	1,141	324	572.2	.000287		550	Local flutter, static S-shape prior to flutter
39	3.6	26.83	.365	1,153	316	567.6	.000303		283	Full-sail flutter evolving from local flutter
40	2.8	4.67	.148	1,162	310	563.5	.000316		350-400	Full-sail flutter, large amplitude, evolving from local flutter
41	7.4	196.18	.690	1,133	808	584.9	.000642		≈600	Local flutter starboard side
42	5.1	140.1	.558	1,147	789	580.2	.000683		≈457	Local flutter both sides
43	4.6	73.98	.392	1,158	765	575.2	.000718		225	Local flutter both sides
44	4.3	17.70	.186	1,166	748	570.3	.000750		145	Full-sail flutter evolving from local flutter, large amplitude on both sides
45	7.0	200.38	.518	1,147	1,284	575.8	.001137		≈480	Local flutter, both sides at leading edge of positive cambered portion of sail
46	6.6	202.06	.520	1,148	1,285	578	.001134			Local flutter, both sides at leading edge (50 percent chord) of positive cambered portion of sail
47	4.0	126.08	.400	1,156	1,257	573.5	.001177			Local flutter
48	2.9	28.04	.183	1,163	1,225	567.1	.001238		260	Full-sail flutter, large amplitude

<sup>f</sup>The sail had no apparent wrinkles at the start of the tests. At the conclusion of the test, the sail cloth had stretched approximately 1/2 inch normal to the center of the sail (in the down direction) and the seams along the cables at the leading edge were frayed. The leading-edge spar fairings were also missing.

CONFIDENTIAL

CONFIDENTIAL

TABLE III.- FLUTTER TEST RESULTS - Continued

(a) Small-model tests - Continued

Run	Angle of attack, $\alpha$ , deg	$q$ , lb/sq ft	Mach number	$a$ , ft/sec	$P_t$ , lb/sq ft	$T_t$ , Or	$\rho$ , slugs/cu ft	Flutter frequency, cps		Remarks
								Sail	Spar	
Model 76; teflon, cable tension										
65	4.2	51.17	0.824	1,102	168	573.0	0.000124	260	260	Local flutter, starboard side
66	4.2	46.62	.763	1,115	167	576.1	.000129	250	250	Local flutter, starboard side
67	3.9	39.30	.678	1,126	164	575.2	.000134	240	240	Local flutter, both sides from 0 to 20 percent of root chord
68	3.3	24.29	.508	1,143	160	571.1	.000144	110	225	Full-sail flutter
69	3.2	11.17	.333	1,156	155	568.0	.000151			Full-sail flutter in negative camber
70	2.0	.93	.093	1,163	155	563.5	.000160			Static reversal
71	4.6	105.89	.831	1,114	343	586.2	.000247	350	350	Local flutter, high frequency, near second inflection point at 80 percent root chord; sail assumes S-shape
72	3.9	81.14	.690	1,132	333	583.0	.000266	259	259	Local flutter, high frequency, near second inflection point at 80 percent root chord; sail assumes S-shape
73	4.0	52.13	.527	1,147	322	577.1	.000285	420	420	Local flutter, high frequency, near second inflection point at 80 percent root chord; sail assumes S-shape
74	3.6	52.13	.527	1,147	322	576.7	.000285	~367	~367	Sail flutter, rear portion; fluttering between positive and zero camber
75	3.9	26.84	.365	1,158	315	572.6	.000300	~300	~300	Local flutter, high frequency, near second inflection point at 80 percent root chord; sail assumes S-shape
76	3.6	26.85	.366	1,158	314	572.2	.000299	~300	~300	Sail flutter, rear portion; fluttering between positive and zero camber
77	2.9	4.66	.149	1,166	308	569.0	.000311	460	460	Sail flutter, low frequency 20 to 100 percent root chord
78	3.5	202.45	.711	1,136	798	590.7	.000621	460	460	Local flutter, sail takes on S-shape, local flutter on leading edge of rear positive camber
79	3.1	126.85	.535	1,153	769	584.3	.000667	450	450	Flutter, intermittent sail flutter; from local to full-sail flutter
80	3.0	72.20	.391	1,161	748	577.1	.000700	467	467	Local flutter, at leading edge of rear positive cambered portion of sail, high-frequency flapping
81	2.8	72.20	.391	1,161	748	577.1	.000700	300-500	300-500	Full-sail flutter, intermittent
82	1.9	15.75	.178	1,168	732	572.6	.000733	300	300	Full-sail flutter, intermittent
83	3.2	206.47	.525	1,154	1,287	583.4	.001125	500	500	Full-sail flutter, local to full sail
84	2.8	123.67	.395	1,163	1,262	580.2	.001172	550	550	Full-sail flutter, local to full sail
85	2.0	26.86	.179	1,169	1,230	574.4	.001227	350	350	Full-sail flutter

<sup>5</sup>The model was found to be severely damaged after the tests; the compression spar was broken at the sail spar juncture, and both leading-edge spar fairings were missing as well as the trailing-edge spar fairings on the port side. The sail was frayed along both leading edges and had considerable slack.

CONFIDENTIAL

TABLE III.- FLUTTER TEST RESULTS - Continued

(a) Small-model tests - Continued

Run	Angle of attack, $\alpha$ , deg	$q$ , lb/sq ft	Mach number	$a$ , ft/sec	$P_t$ , lb/sq ft	$T_t$ , OR	$\rho$ , slugs/cu ft	Flutter frequency, cps		Remarks
								Sail	Spar	
Model 8 <sup>h</sup> , teflon, no cable tension										
119	3.5	67.53	1.169	508	183	535.7	0.000383	200	200	Local flutter.
120	2	38.96	.772	516	160	526.0	.000491	~450	~450	Full-sail flutter, camber almost eliminated before flutter reversal
121	2.3	26.78	.609	516	157	520.1	.000542	383	383	Local flutter; S-shape with detached negative-cambered portion approximately 1/4 inch from tip of mast
121	2.1	26.78	.607	516	158	520.1	.000546			Full-sail flutter; sail reverses camber
122	1.7	5.52	.258	522	152	519.8	.000609			Static reversal; small vibration prior to reversal
123	4.7	151.51	1.170	506	414	548.9	.000865	500	500	Local flutter; port side only, negative cambered portion of S-shaped sail 1/4 inch from tip of mast
124	2.6	92.81	.807	513	360	535.7	.001083	210	210	Full-sail flutter; sail reverses camber
125	2.3	57.22	.595	515	349	530	.001220	~75	~75	Full-sail flutter; negative-cambered portion approximately 1/2 inch from tip of mast
126	1.5	14.74	.284	517	340	526.4	.001367	65	65	Full-sail flutter
127	2.6	189.17	.775	501	778	529.5	.002507	925	925	Local flutter, largest amplitudes at negative-cambered portion of sail
128	2.7	125.55	.600	504	757	527.8	.002744	500	500	Local flutter, intermittent
129	2.0	61.32	.402	506	740	525.0	.002964	167	167	Full-sail flutter; detached negative-cambered portion of sail back 3/4 inch
130	1.7	32.03	.286	506	732	523.3	.003059	120	120	Full-sail flutter
131	2.8	189.30	.577	492	1,218	513.2	.004706			Local flutter
132	2.2	98.51	.409	494	1,153	512.4	.004838			Local flutter
133	1.5	38.46	.254	494	1,107	510.1	.004905			Local flutter

<sup>h</sup>The sail tension appeared to be uniform before and after the tests.



CONFIDENTIAL

TABLE III.- FLUTTER TEST RESULTS - Continued

(a) Small-model tests - Continued

Run	Angle of attack, $\alpha$ , deg	q, lb/sq ft	Mach number	a, ft/sec	P <sub>t</sub> , lb/sq ft	T <sub>t</sub> , or P <sub>t</sub> , lb/sq ft	$\rho$ , slugs/cu ft	Flutter frequency, cps		Remarks
								Sail	Spar	
Model 9 <sup>1</sup> ; rubberized nylon, no cable tension										
18	2.4	54.18	0.855	1,094	170	569.9	0.000124	54.87		Full-sail flutter
19	2.4	40.72	.681	1,120	170	569.5	.000140	350		Full-sail flutter, intermittent
20	2.2	23.90	.491	1,140	165	566.2	.000150	330		Full-sail flutter, sail deflected down into negative camber
21	1.8	12.08	.339	1,150	163	562.2	.000159			Sail deflected down, negative camber, then fluttered upward with low amplitude
21	3.8	115.13	.833	1,113	374	585.7	.000268	666		Angle necessary to change from negative to positive camber
22	5.7									Sail flutter, starboard side only; starboard side appears to have more camber
23	4.0	88.87	.692	1,131	363	583	.000290	550		Sail flutter, starboard side only
24	2.3	57.93	.536	1,147	351	578	.000307	410		Sail flutter, static S-shape before flutter, sail in negative camber at flutter
25	2.1	29.58	.370	1,154	340	569	.000325			Sail deflected down, negative camber
25	3.4									Angle necessary to change from negative to positive camber
26	7.2	202.38	.697	1,140	813	592.9	.000642	550		Sail flutter, starboard side only; cloth appears to have stretched more on starboard side
27	2.75	139.96	.557	1,157	793	590.7	.000674	520		Sail flutter, leading-edge spar cap loose on port side and missing on starboard side
28	2.3	70.19	.3810	1,163	764	578.9	.000715			Sail deflected down, negative camber
28	4.4									Angle necessary to change camber from negative to positive
29	3.0	211.68	.5321	1,157	1,295	588	.001117			Local-sail flutter, starboard side only
30	3.7	124.6	.395	1,166	1,270	584.3	.001169	250		Sail deflected down, negative camber, low amplitude flutter

<sup>1</sup>The sail was slightly wrinkled at the start of the tests. At the end of the test, the starboard cable was found to be very loose due to the cable slipping the joint at the compression spar.

CONFIDENTIAL

CONFIDENTIAL

21

TABLE III.- FLUTTER TEST RESULTS - Continued

(a) Small-model tests - Continued

Run	Angle of attack, $\alpha$ , deg	$q$ , lb/sq ft	Mach number	$a$ , ft/sec	$P_t$ , lb/sq ft	$T_t$ , OR	$\rho$ , slugs/cu ft	Flutter frequency, cps		Remarks
								Sail	Spar	
Model 10 <sup>1</sup> ; rubberized nylon, cable tension										
49	2.8	50.79	0.854	1,078	160	553.2	0.00120	400-500	400-500	Full-sail flutter; verge of reversal
50	2.8	44.19	.763	1,094	158	554.2	.000127	450	466	Full-sail flutter, intermittent tendency to reverse, angle critical
51	2.7	37.86	.690	1,102	156	552.0	.000131	325	400-500	Full-sail flutter, oscillating between zero and negative camber
52	2.6	24.16	.519	1,120	154	548.9	.000143	325	325	Full-sail flutter, negative camber; local flutter before sail reversed
53	5.1	24.23	.518	1,120	155	549.3	.000144	300	325	Angle necessary to go from negative to positive camber
54	3.0	10.29	.321	1,135	153	546.7	.000155	300	325	Local flutter before reversal; then sail flutter about negative camber
55	4.5	109.23	.852	1,095	344	569.5	.000251	500	500	Angle necessary to go from negative to positive camber
56	3.2	79.24	.683	1,116	331	565.4	.000273	483	483	Local flutter at inflection between forward negative camber and aft positive camber, intermittent
57	2.4	52.62	.530	1,128	325	559.7	.000295	~15	~15	Local flutter, large amplitude, same static S-shape as above with positive cambered portion 50 to 100 percent of root chord
58	3.1	28.75	.377	1,142	319	557.2	.000311	317	317	Sail flutter, 0 to 20 percent chord billowed up; 20 to 100 percent down; severe flutter of rear portion
59	2.6	4.65	.147	1,153	313	554.7	.000324	500	500	Angle necessary to change rear camber from negative to positive
60	4.4	212.63	.737	1,120	800	577.1	.000625	-----	-----	Sail flutter, 0 to 20 percent chord billowed up; 20 to 100 percent down; reverse flutter of rear portion
61	2.4	125.89	.532	1,139	727	569.9	.000687	-----	-----	Angle necessary to change rear camber from negative to positive
62	4.9	70.30	.384	1,150	754	564.5	.000721	-----	-----	Static instability
63	2.5	209.13	.530	1,142	1,288	572.6	.001143	430	430	Angle necessary to change camber from negative to positive
64	1.3	115.02	.381	1,152	1,256	568.0	.001194	-----	-----	Local flutter, at forward negative camber portion of sail; rear 50 percent of sail has positive camber
65	2.2	29.79	.189	1,160	1,229	563.5	.001248	275	275	Static instability, change of chord shape from S-shape to negative camber over whole sail
66	1.1	29.79	.189	1,158	1,227	562.2	.001248	-----	-----	Static instability, change of chord shape from S-shape to negative camber over whole sail
67	4.0							-----	-----	Angle necessary to go from negative camber to positive camber
68	1.4							-----	-----	Static instability; violent change of S-shape to negative camber; inflection point at 60 percent root chord when reversal occurred
69	2.4							-----	-----	Static instability; short intermittent bursts of flutter in region at inflection; no change in $\alpha$ when reversal occurred
70	1.4							-----	-----	Angle necessary to go from negative to positive camber
71	3.8							-----	-----	Static instability, as in run 62
72	5.1							-----	-----	Angle necessary to change from negative to positive camber
73								-----	-----	Static instability, as in run 62
74								-----	-----	Angle necessary to change from negative to positive camber

<sup>1</sup>This model was the same as model 9 except that tension had been added to the cable and the leading-edge spar fairings were removed. There was a wrinkle in the sail at the midchord before the test. At the conclusion of the test the seams along the cables at the leading edge were frayed. The trailing-edge spar fairings were also missing.

CONFIDENTIAL

CONFIDENTIAL

TABLE III.- FLUTTER TEST RESULTS - Continued

(a) Small-model tests - Concluded

Run	Angle of attack, $\alpha$ , deg	$q$ , lb/sq ft	Mach number	$a$ , ft/sec	$P_t$ , lb/sq ft	$T_t$ , OR	$\rho$ , slugs/cu ft	Flutter frequency,		Remarks
								cps		
								Sail	Spar	
Model 11 <sup>k</sup> , fiberglass, no cable tension										
153	7.5	146.10	1.162	520	402	569.9	0.000801	533		Local flutter, sail billow approximately 3/8 inch
154	4.9	119.87	.986	524	371	563.5	.000899	333		Local flutter, sail billow approximately 3/8 inch and fraying at trailing edge
155	6.0	86.44	.779	526	353	554.7	.001031	450		Local flutter, fraying at trailing edge
156	4.6	55.40	.588	529	344	549.8	.001144			Local flutter, fraying at trailing edge
157	3.9	24.49	.374	531	335	545.8	.001243			Local flutter, fraying at trailing edge

<sup>k</sup>The sail started to fray at the start of the test along the trailing edge of the sail and the tests were terminated after the sail had frayed approximately 50 percent of the length of the spars.

CONFIDENTIAL

CONFIDENTIAL

CONFIDENTIAL

23

TABLE III.- FLUTTER TEST RESULTS - Continued

(b) Large-model tests

Run	Angle of attack, $\alpha$ , deg	$q$ , lb/sq ft	Mach number	$s$ , ft/sec	$P_t$ , lb/sq ft	$T_t$ , OR	$\rho$ , slugs/cu ft	Flutter frequency of spar, cps	Remarks
Model 12; nylon, no cable tension									
1	8.25	79.4	1.87	872.54	226	538	$0.5985 \times 10^4$		Local flutter, over 50 to 60 percent of rear portion of sail, both panels
2	7.70	80.2	1.87	873.79	229	540	.6043		Local flutter as above with larger amplitude over both panels, large area
3	9.36	91.5	1.88	874.35	261	543	.6774	240	Local flutter most evident on starboard side
4	8.71	91.4	1.88	876.76	260	544	.6735	210	Local flutter, larger amplitude, stitching along cable coming out on both panels
5	10.23	101.6	1.89	874.81	289	546	.7376	$\approx 256$	Local flutter, most evident on starboard side
6	11.58	111.2	1.90	876.05	316	550	.7921	$\approx 250$	Local flutter, sail billow increasing; flutter about $4\frac{1}{2}$ inches from tip of fuselage along leading edge of billow
Model 13 <sup>1</sup> ; nylon, no cable tension									
1	12.96	81.3	1.87	865.66	232	530	$0.6144 \times 10^4$	225	Local flutter, both sails; 60 to 100 percent of port sail, port boom vibrating; both panels
2	10.47	80.8	1.87	867.29	230	532	.6160	213	Local flutter, both sails; hole in starboard sail near spar and 1 inch from tip of spar
3	13.60	91.4	1.88	867.07	260	534	.6861	237	Local flutter, port sail
4	15.60	100.7	1.89	865.96	286	535	.7450	258	Local flutter, port sail; hole no larger in starboard sail
5	16.63	109.8	1.90	864.83	312	536	.8025	257	Local flutter, port sail; hole no larger in starboard sail
6	15.00	81.7	1.87	881.84	233	550	.6035	237	Local flutter, hole in port sail along boom, hole increasing in size on starboard sail
7	8.00	82.2	1.87	882.65	234	551	.6050		Local flutter, deep into flutter region; same type of flutter with greater amplitude

<sup>1</sup>The model was destroyed in the subsonic flow after the tests.

CONFIDENTIAL

CONFIDENTIAL

TABLE III.- FLUTTER TEST RESULTS - Concluded

## (b) Large-model tests - Concluded

Run	Angle of attack, $\alpha$ , deg	$q$ , lb/sq ft	Mach number	$a$ , ft/sec	$P_t$ , lb/sq ft	$T_t$ , OR	$\rho$ , slugs/cu ft	Flutter frequency of spar, cps	Remarks
Model 14; teflon, cable tension									
1	6.37	80.4	1.87	870.55	229	536	$0.6087 \times 10^4$	286	Local flutter, both sails from approximately 35 to 100 percent root chord
2	5.98	81.0	1.87	871.36	231	537	.6128		Local flutter, larger amplitude; both sails from approximately 35 to 100 percent root chord
3	6.70	90.1	1.88	871.93	252	540	.6576		Local flutter, both sails from approximately 35 to 100 percent root chord
4	6.45	90.8	1.88	873.54	259	542	.6735	300	Local flutter, larger amplitude
5	7.05	102.5	1.89	874.81	292	546	.7453		Local flutter, both sails from approximately 35 to 100 percent root chord
6	6.58	102.3	1.89	875.61	291	547	.7414	500	Local flutter, larger amplitude
7	7.27	111.2	1.90			550	.7921		Local flutter, both sails from approximately 35 to 100 percent root chord
8	7.04	111.2	1.90	876.05	316				
Model 15 <sup>m</sup> ; rubberized nylon, no cable tension									
1	7.66	81.1	1.87	868.92	231	534	$0.6162 \times 10^4$	350	Local flutter, starboard sail, at leading edge of sail near cable and at tip of fuselage
2	6.75	81.3	1.87	869.73	232	535	.6180		Local flutter, starboard sail, at leading edge of sail near cable and at tip of fuselage; increased amplitude
3	8.97	90.8	1.88	871.93	259	540	.6760	427	Local flutter, same as run 1
4	7.56	91.2	1.88		260				Local flutter, starboard sail, at leading edge of sail near cable and at tip of fuselage
5	7.83	102.5	1.89	874.01	292	545	.7467	200-400	Local flutter as in preceding runs
6	8.16	110.3	1.90	875.26	314	549	.7895	380-400	Local flutter as in preceding runs
7	7.00	110.3	1.90	876.05	314	550	.7872		Local flutter, same as run 6, increased amplitude
Model 16 <sup>n</sup> ; rubberized nylon, no cable tension									
1	6.15	80.4	1.87	873.79	229	540	$0.6043 \times 10^4$	400	Local flutter, slight motion on starboard cable and fabric near cable
2	5.80	80.6	1.87	875.41	230	542	.6045		Local flutter - sustained flutter on starboard cable, slight motion on port cable
3	6.72	90.7	1.88	875.96	258	545	.6671		Local flutter, stitching coming out along cable on both sides, 30 to 100 percent of leading edge
4	5.98	90.3	1.88	876.76	257	546	.6634	250-300	Sail ripped

<sup>m</sup>The model was destroyed in the turbulent subsonic flow after the tests.<sup>n</sup>The model was destroyed in the subsonic flow after the tests.

CONFIDENTIAL

DECLASSIFIED

CONFIDENTIAL

25

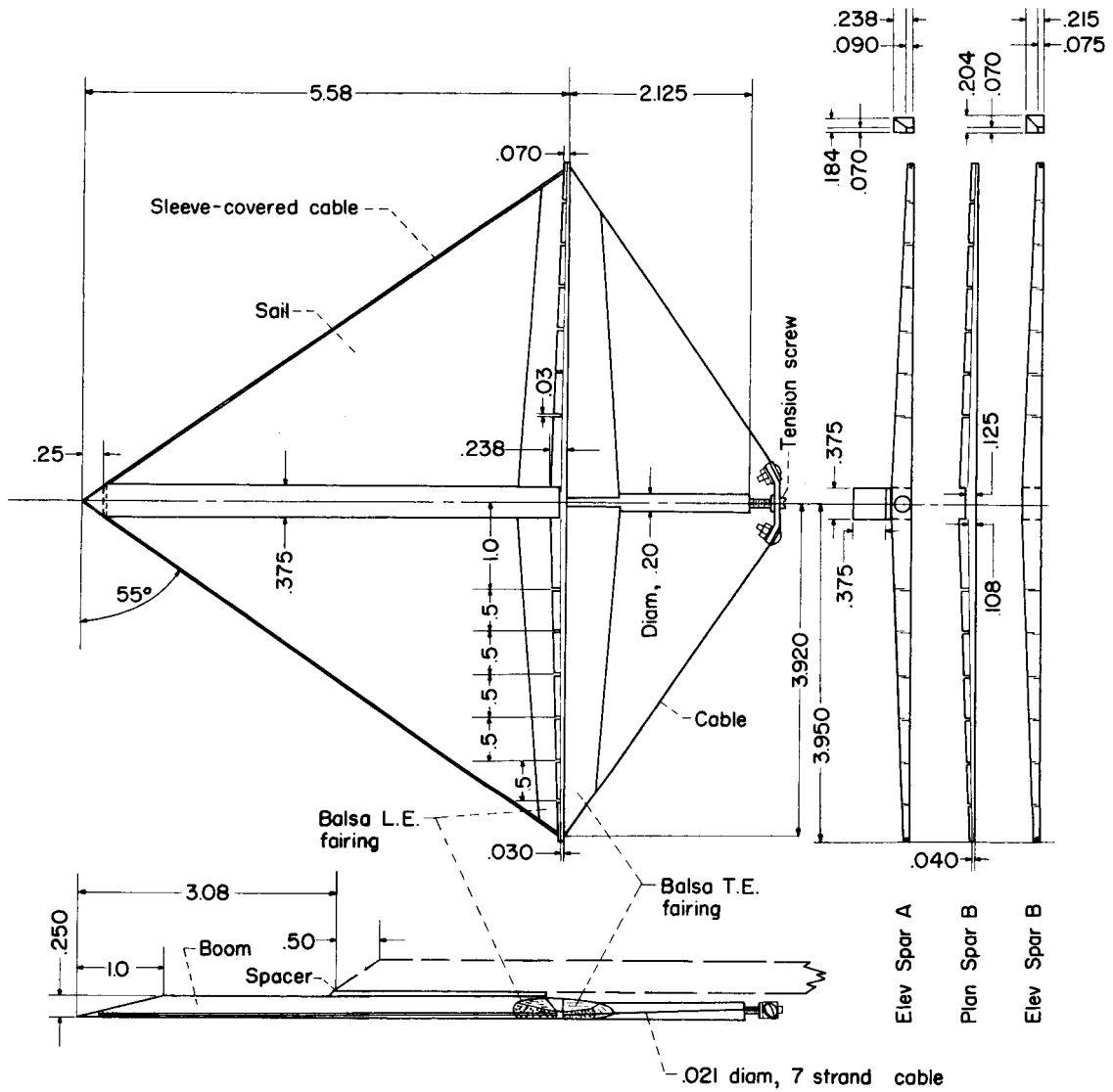


Figure 1.- Detail drawing of small model. Dimensions are in inches.

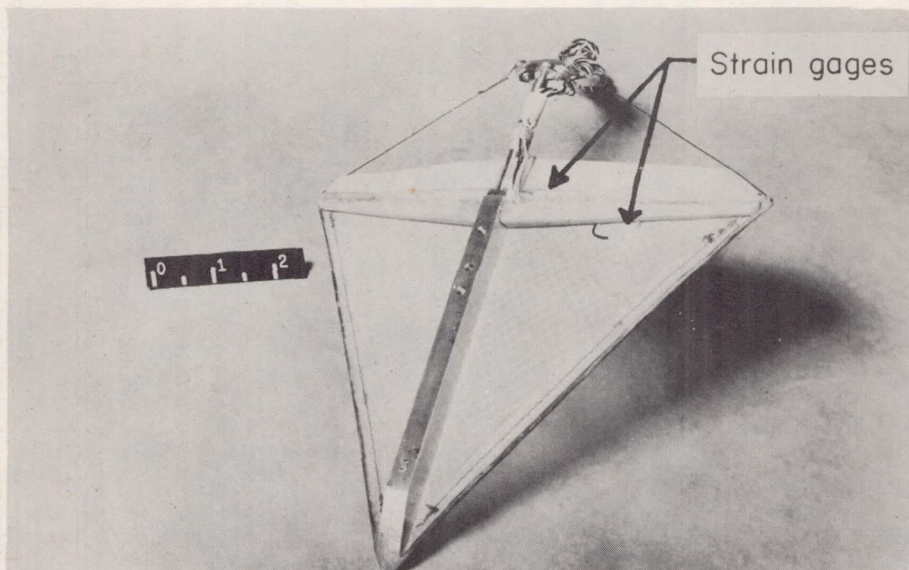
CONFIDENTIAL



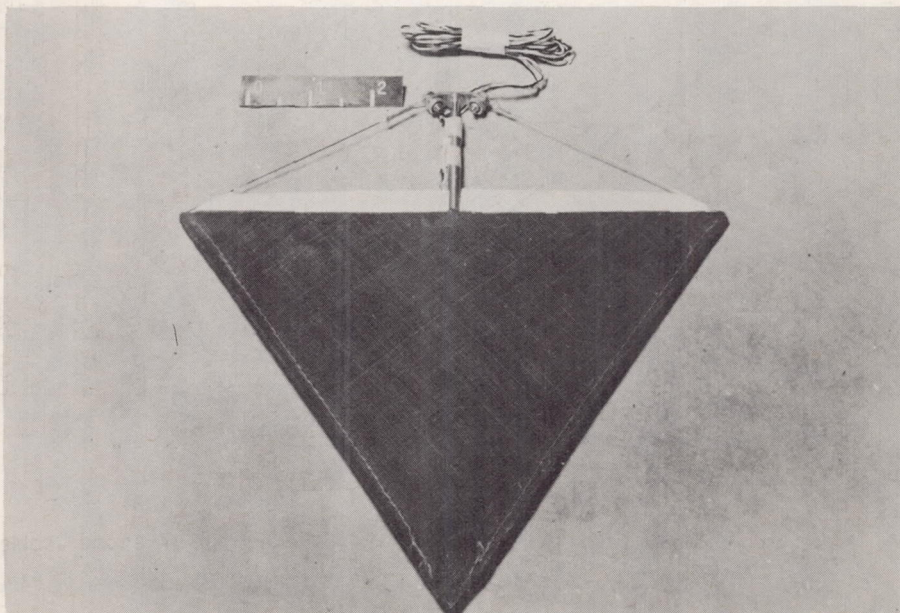
031710201030

26

CONFIDENTIAL



(a) Top view of nylon-covered model.



(b) Bottom view of Teflon-covered model.

L-60-4334

Figure 2.- Top and bottom views of small models.

CONFIDENTIAL

CONFIDENTIAL

The drawing includes the following labels and dimensions:

- Plan View (Top):**
  - Overall length: 9.207
  - Distance from bow to mast: 3.875
  - Mast diameter: Diam. .3125
  - Boom diameter: .045
  - Angle at bow: 55°
  - Labels: Sleeve-covered cable, Sail, Balsa L.E. fairing, Cable, Tension screw, Balance housing, R=0.500
  - Dimensions for sail and boom: .250, .500, .170, .121, .045
- Elevation View (Bottom):**
  - Labels: Balance housing, Boom, Compression spar, Balsa T.E. fairing
  - Dimensions: 10, 250, 3.375, 5.94, .375
- Section Views (Right):**
  - Elev Spar A:** Dimensions .364, .135, .289, .105, .875, 10.62, 6.468, 6.50, .50, .165, .055
  - Plan Spar B:** Dimensions .329, .109, .319, .105
  - Elev Spar B:** Dimensions .329, .109, .319, .105
- Other Labels:**
  - .031 diam, 17 strand cable

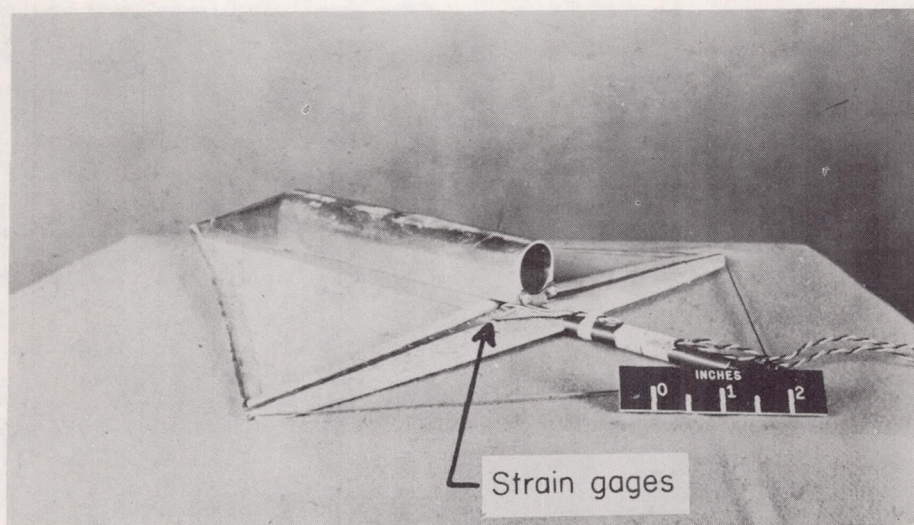
CONFIDENTIAL



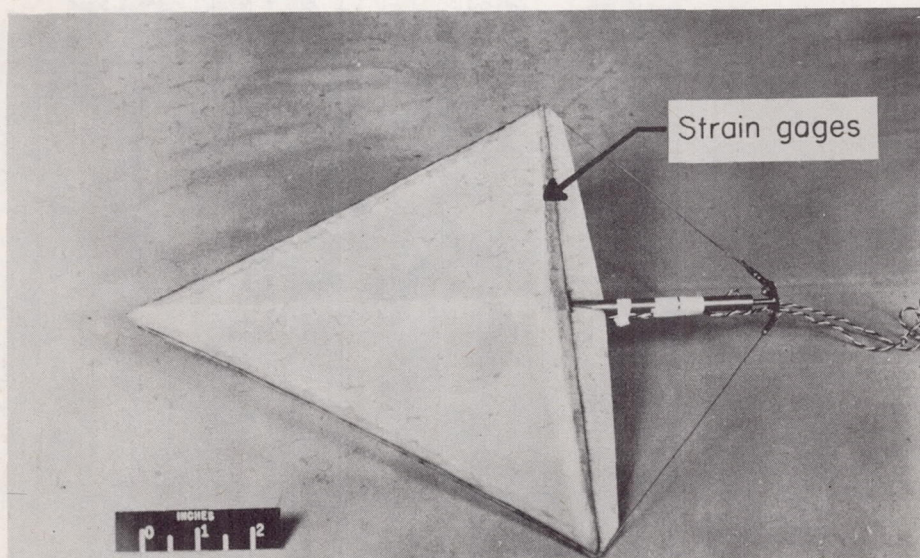
03710281030

28

CONFIDENTIAL



(a) Top view.



(b) Bottom view.

L-60-4335

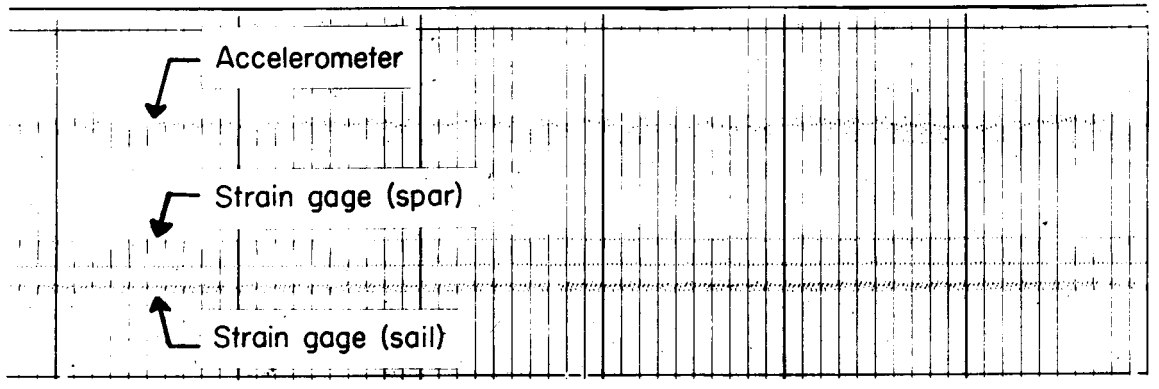
Figure 4.- Top and bottom views of large model.

CONFIDENTIAL

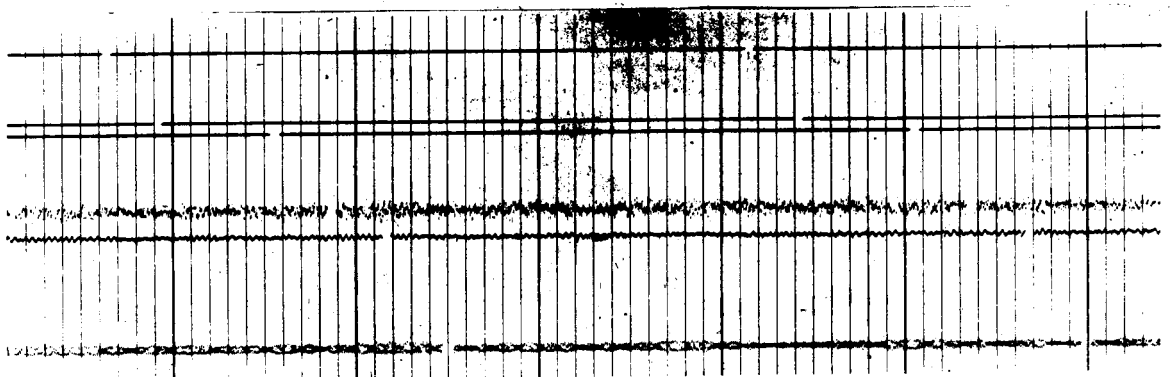
DECLASSIFIED

CONFIDENTIAL

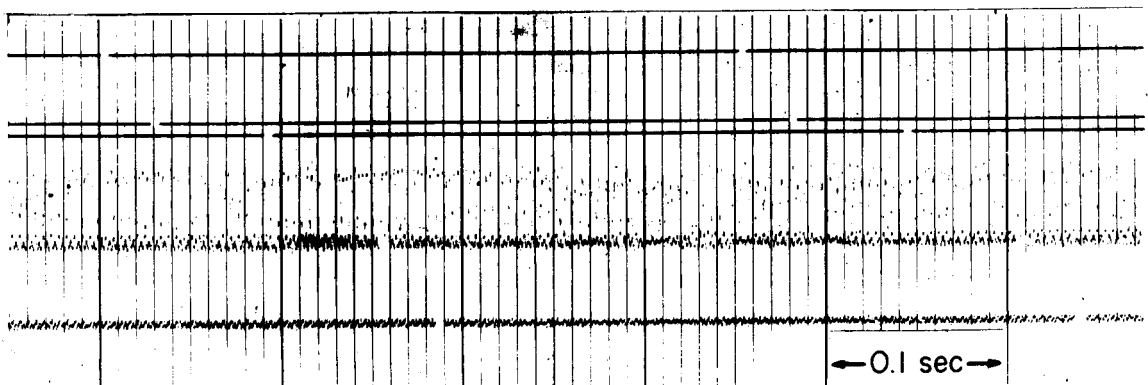
29



(a) Full-sail flutter; model 3, run 146.



(b) Local flutter; model 2, run 98.



(c) Local flutter; model 7, run 67.

Figure 5.- Sample records taken during large model tests.

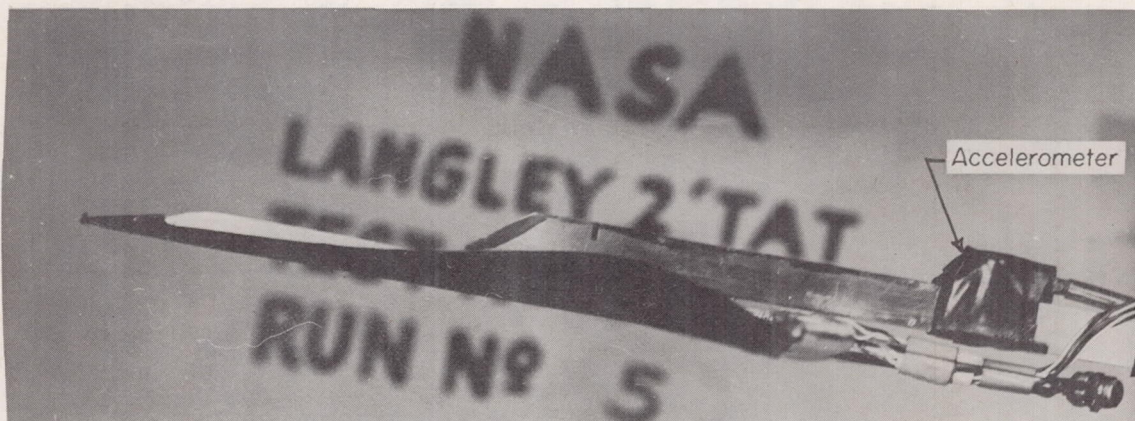
CONFIDENTIAL



031710201030

30

CONFIDENTIAL



(a)  $\alpha_{\text{photograph}} = 9.5^\circ$ ;  $\alpha_{\text{flutter}} = 4.2^\circ$ ;  $M = 0.81$ ;  $q = 49.23 \text{ lb/sq ft.}$



L-60-4336

(b)  $\alpha_{\text{photograph}} = 3.3^\circ$ ;  $\alpha_{\text{flutter}} = 3.2^\circ$ ;  $M = 0.333$ ;  $q = 11.2 \text{ lb/sq ft.}$

Figure 6.- Variation in camber with angle of attack and dynamic pressure for small model 7.

CONFIDENTIAL

DECLASSIFIED

CONFIDENTIAL

31

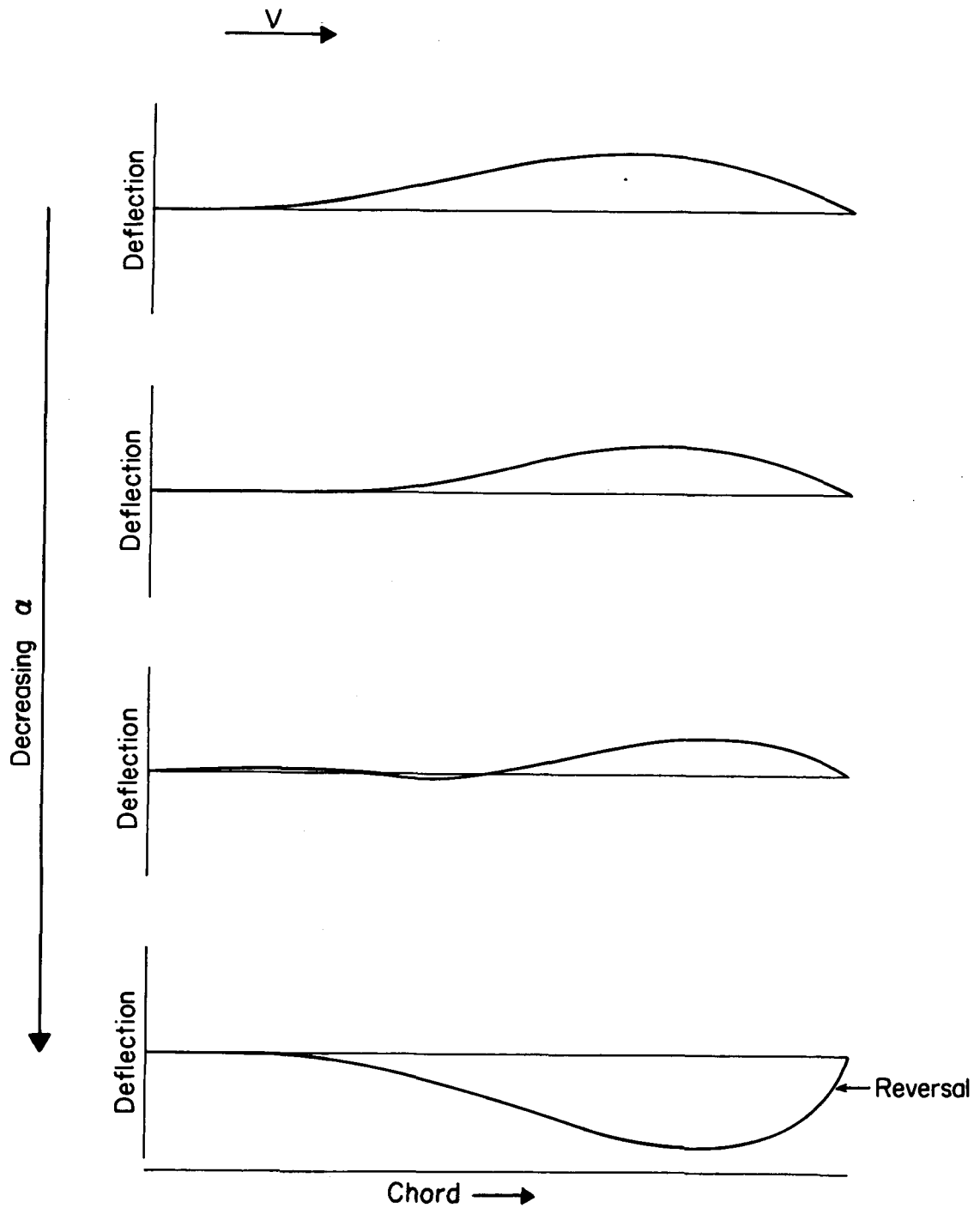
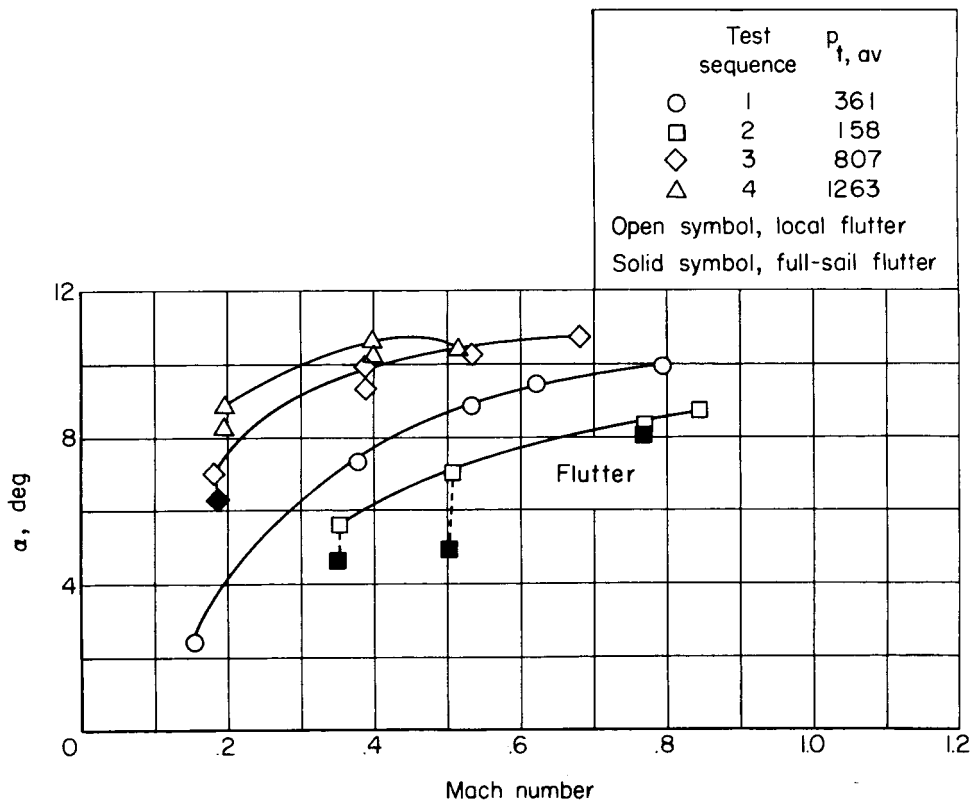
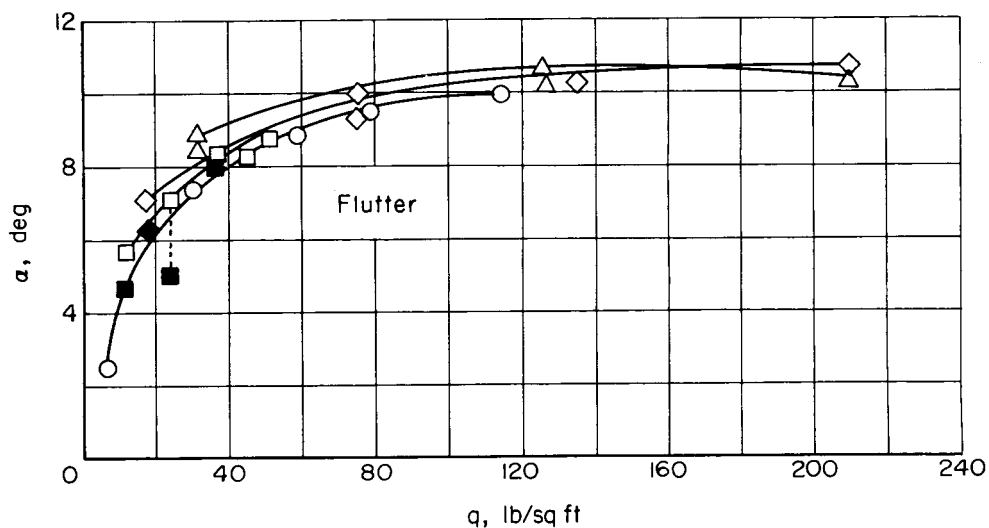


Figure 7.- Schematic drawing of changes in camber during small model tests.

CONFIDENTIAL



03:13:20.1030



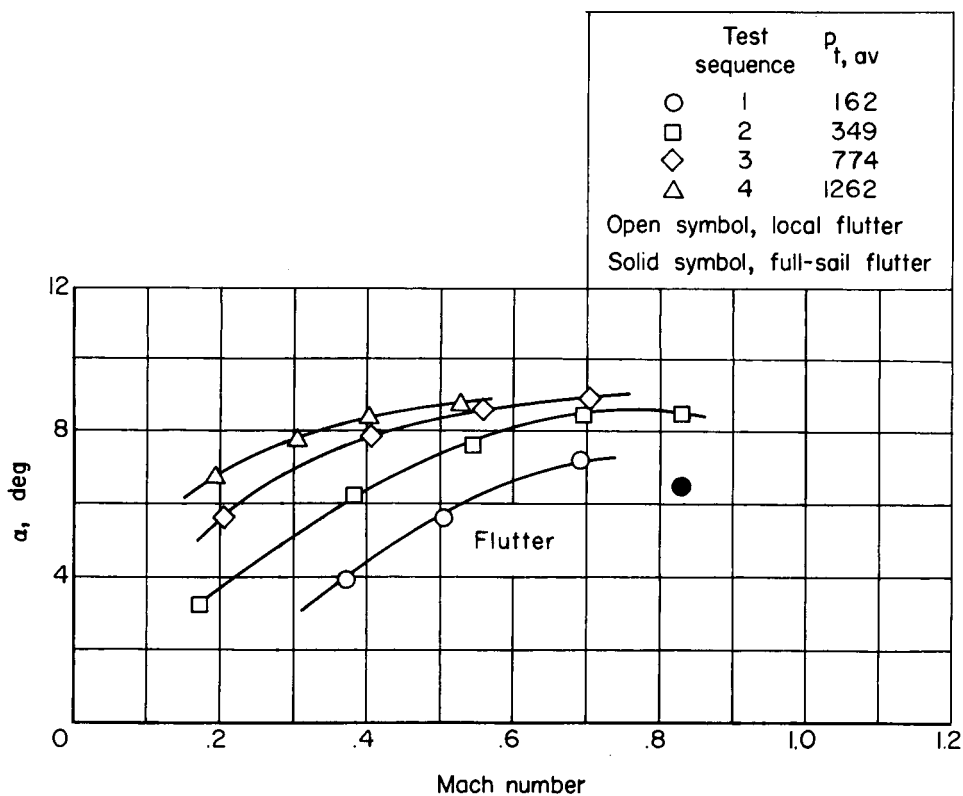
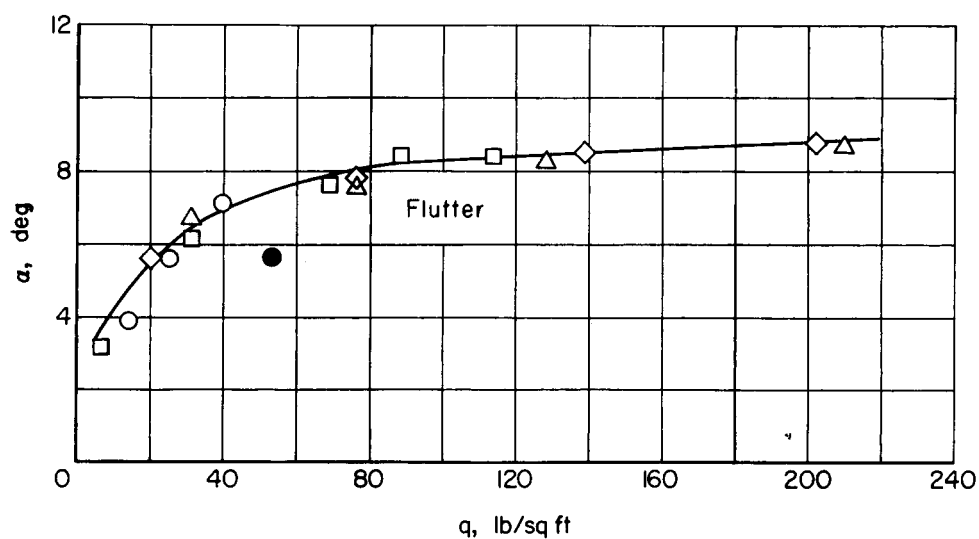
(a) Model 1.

Figure 8.- Variation of angle of attack, at instability, with dynamic pressure and Mach number for small nylon-covered models.

# DECLASSIFIED

CONFIDENTIAL

33



(b) Model 2.

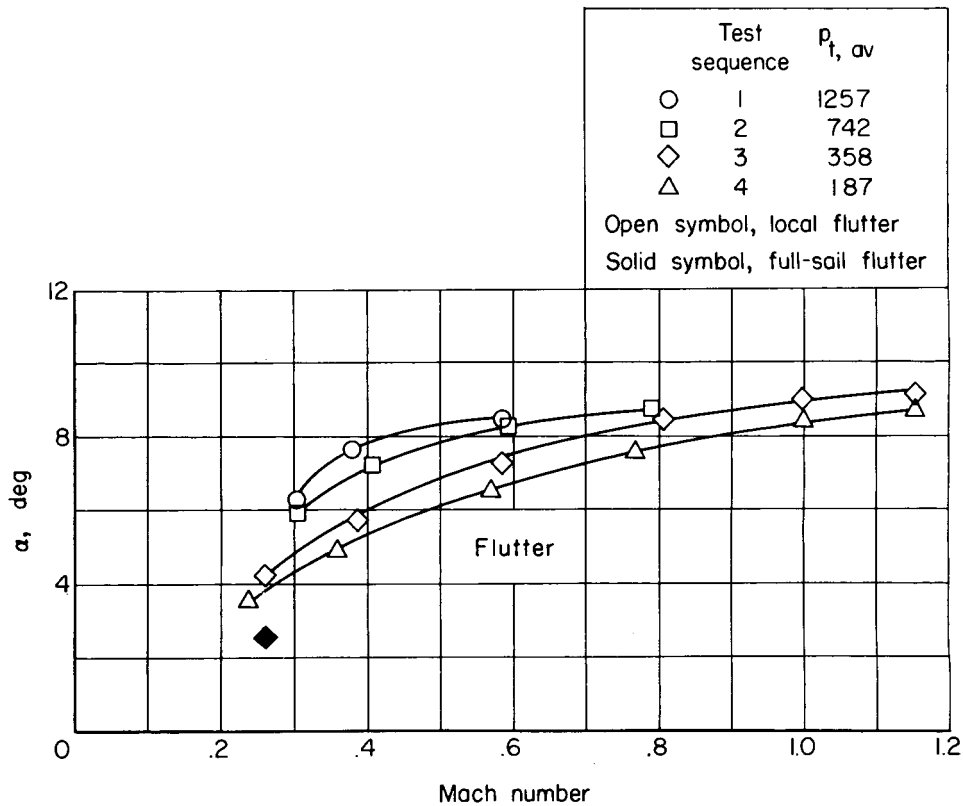
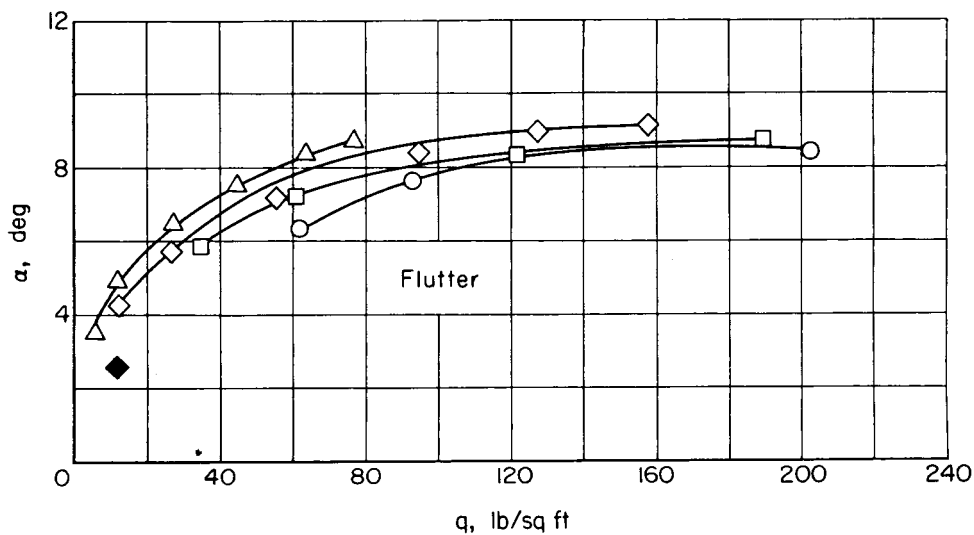
Figure 8.- Continued.

CONFIDENTIAL

031715201030

34

CONFIDENTIAL



(c) Model 3.

Figure 8.- Concluded.

CONFIDENTIAL

# DECLASSIFIED

CONFIDENTIAL

35

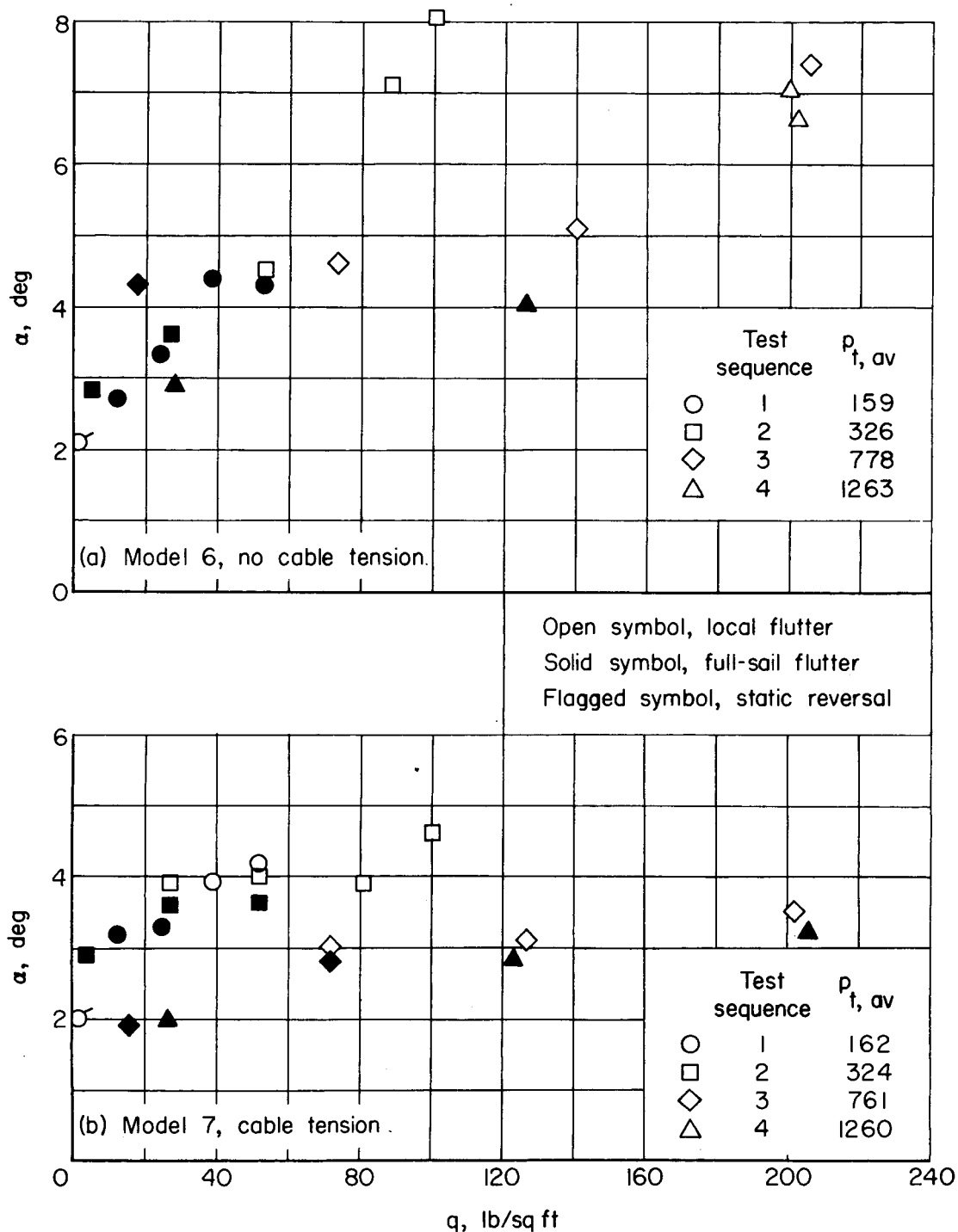


Figure 9.- Variation of angle of attack, at instability, with dynamic pressure for small Teflon covered models.

CONFIDENTIAL

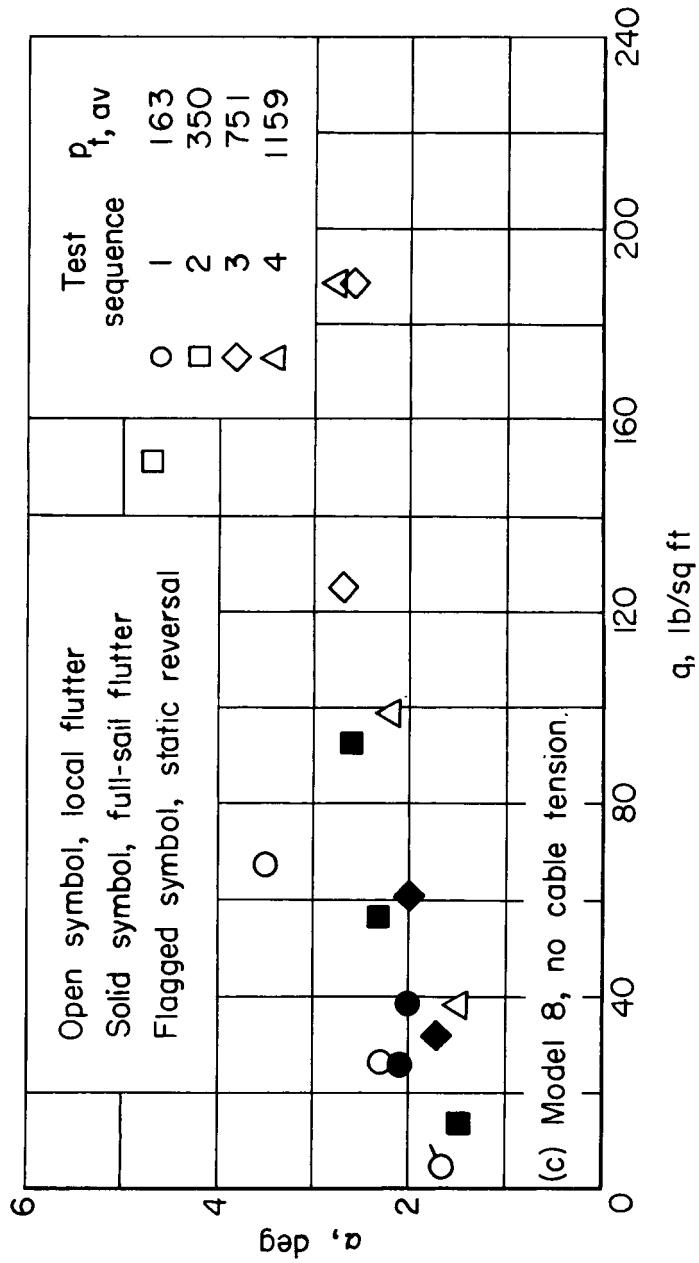


Figure 9.- Concluded.

# DECLASSIFIED

CONFIDENTIAL

37

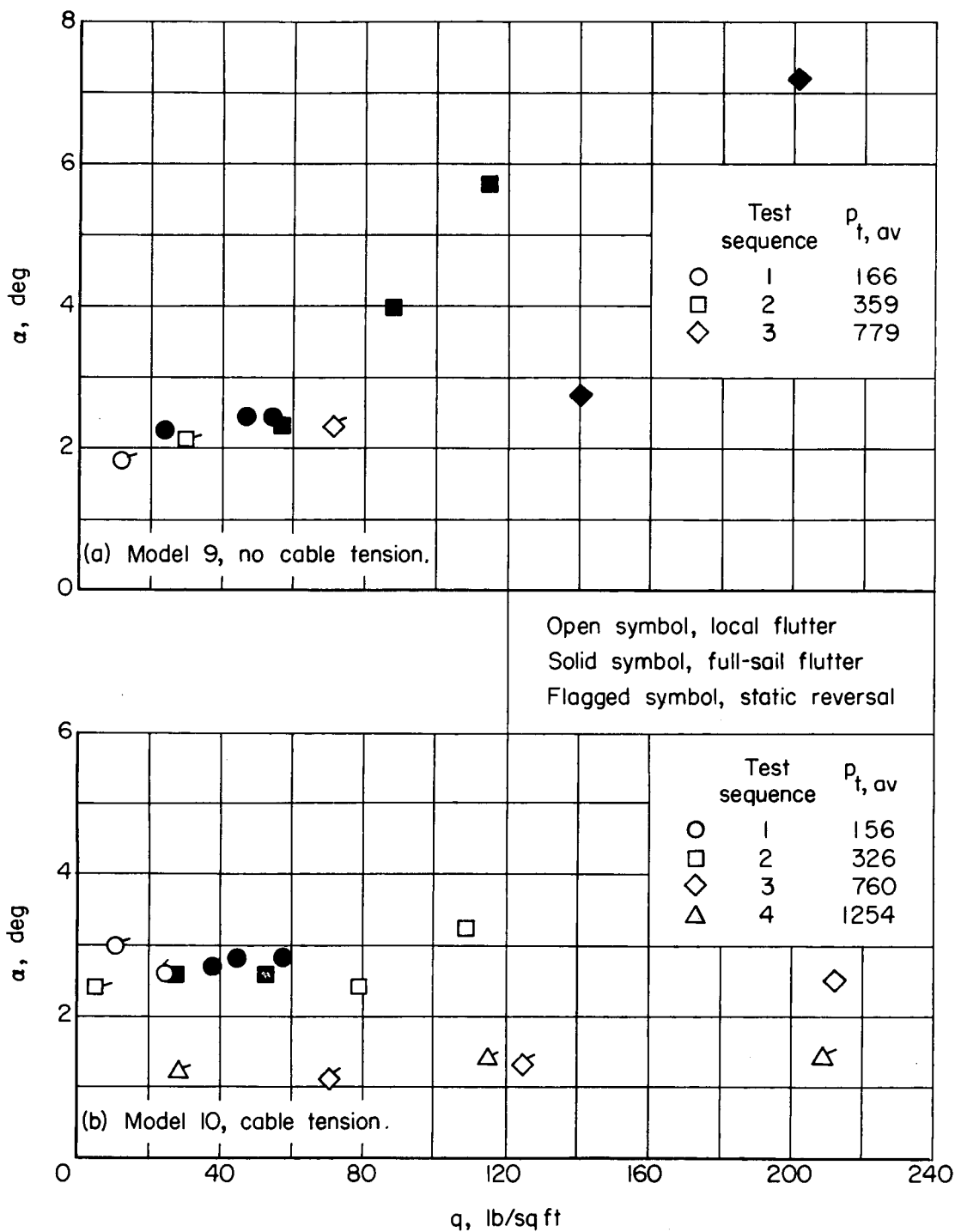


Figure 10.- Variation of angle of attack, at instability, with dynamic pressure for small rubber-coated nylon models.

CONFIDENTIAL

03171320.1030

38

CONFIDENTIAL

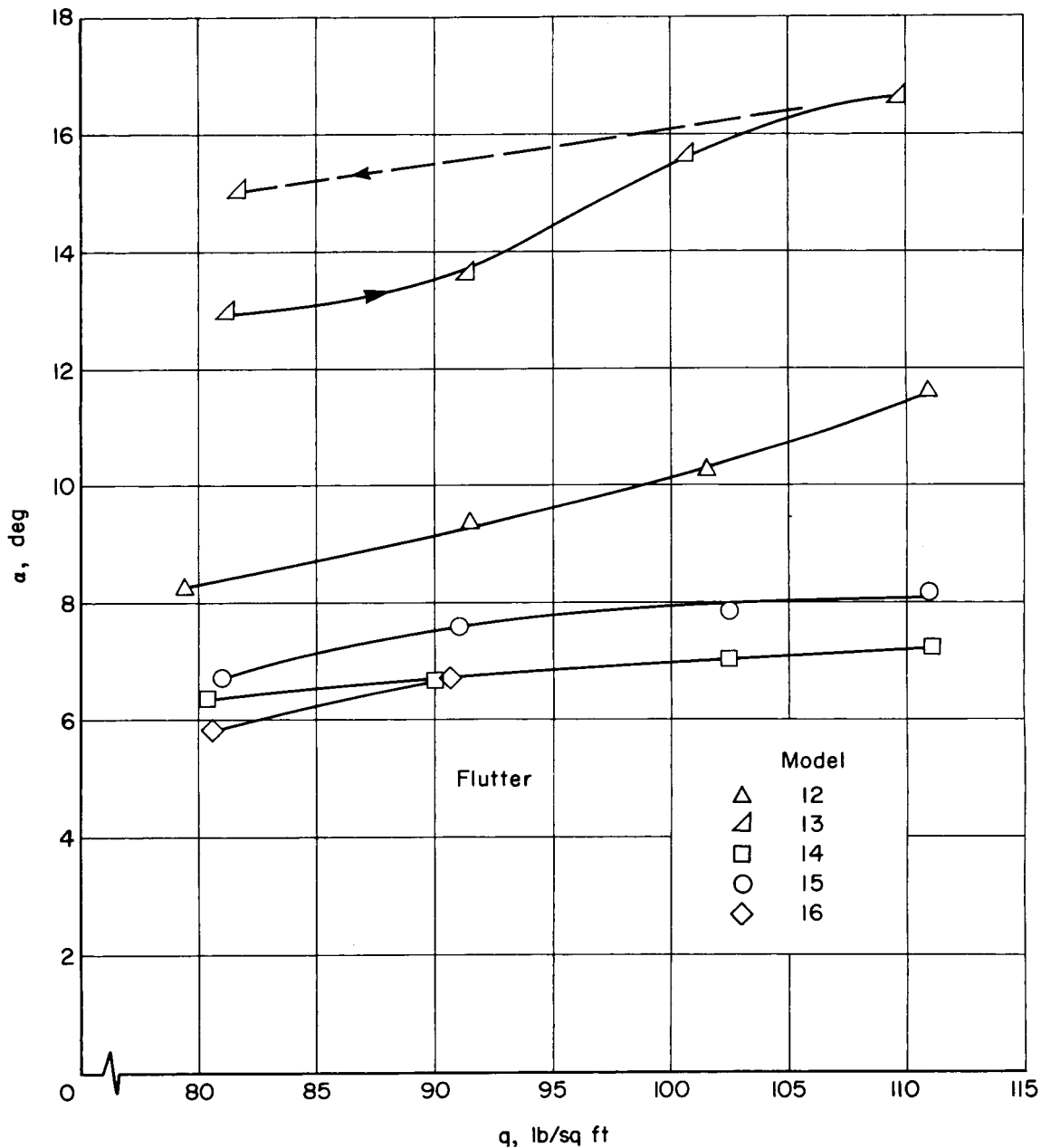


Figure 11.- Variation of angle of attack with dynamic pressure at flutter (local) for large models.  $M = 1.90$ . Arrow indicates sequence of tests.

CONFIDENTIAL

# DECLASSIFIED

CONFIDENTIAL

39

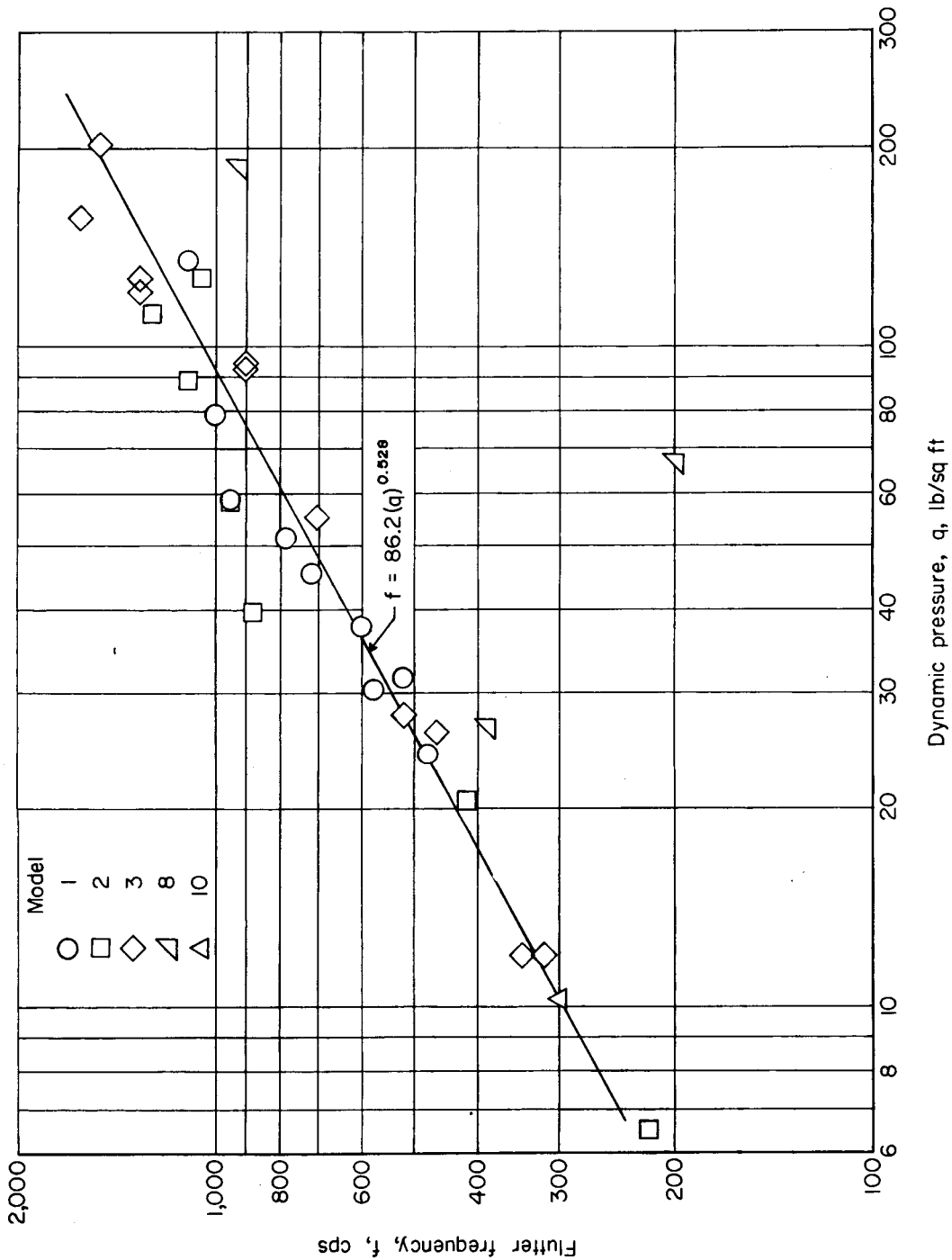


Figure 12.- Local sail flutter frequency (sail strain gages) of small models as a function of dynamic pressure.



DECLASSIFIED

CONFIDENTIAL

CONFIDENTIAL